Immunology and Inflammation

Amphibian mast cells: barriers to deadly chytrid fungus infections

Kelsey A. Hauser, Muhammad R. H. Hossainey, Lindsey K. Gentry, Christina N. Garvey, Netra Ranganathan, Amulya Yaparla, Namarta Kalia, Mira Zelle, Elizabeth J. Jones, Anju N. Duttargi, Louise A. Rollins-Smith, Carly R. Muletz-Wolz, Leon Grayfer

Department of Biological Sciences, The George Washington University, Washington, DC, USA • Center for Conservation Genomics, Smithsonian National Zoo & Conservation Biology Institute, Washington, DC, USA • Department of Oncology, Lombardi Comprehensive Cancer Center, Georgetown University, Washington DC, USA • Departments of Pathology, Microbiology and Immunology, and of Pediatrics, Vanderbilt University School of Medicine, Nashville, TN, USA • Department of Biological Sciences, Vanderbilt University, Nashville, TN, USA

Reviewed Preprint

Published from the original preprint after peer review and assessment by eLife.

About eLife's process

Reviewed preprint version 1
December 19, 2023 (this version)

Posted to preprint server
October 1, 2023

Sent for peer review
September 12, 2023

Abstract

Global amphibian declines are largely driven by deadly disease outbreaks caused by the chytrid fungus, *Batrachochytrium dendrobatidis* (*Bd*). In the time since these disease outbreaks were first discovered, much has been learned about the roles of amphibian skin-produced antimicrobial components and skin microbiomes in controlling *Bd*. Yet almost nothing is known about the roles of skin-resident immune cells in anti-*Bd* defenses. Notably, mammalian mast cells reside within and serve as key immune sentinels in barrier tissues like the skin. Thus, they are critical to immune recognition of pathogens and to orchestrating the ensuing immune responses. Accordingly, we investigated the roles of *Xenopus laevis* frog mast cells during *Bd* infections. Our findings indicate that enrichment of *X. laevis* skin mast cells confers significant anti-*Bd* protection and ameliorates the inflammation-associated skin damage caused by *Bd* infection. Moreover, enriching *X. laevis* mast cells promotes greater mucin content within cutaneous mucus glands and protects frogs from *Bd*-mediated changes to their skin microbiomes. Together, this work underlines the importance of amphibian skin-resident immune cells in anti-*Bd* defenses and introduces a novel approach for investigating amphibian host-chytrid pathogen interactions.

eLife assessment

Overall, this is a significant study, and it is able to highlight mast cells in amphibians and their putative capability to respond to and combat fungal infections. Therefore, this study is **important** for the field. However, the manuscript is **incomplete** from the standpoint that there is functional data lacking on how these mast cells are activated and their precise functional properties. Such experiments would add substantial impact and rigor and fully support the conclusions.

Introduction

Catastrophic declines of hundreds of amphibian species across six continents have been causally linked to the chytrid fungi, *Batrachochytrium dendrobatidis* (*Bd*) and *Batrachochytrium salamandrivorans* (*Bsal*)[1, 2]. Motile *Bd* zoospores readily colonize keratinized skin of adult amphibians and keratinized mouthparts of tadpoles[3]. *Bd* skin infections culminate in chytridiomycosis, ultimately disrupting the function of this respiratory and barrier tissue[3, 4, 5]. Effectively combatting chytrid infections requires a holistic understanding of amphibian cutaneous immune defenses. Research efforts up to this point have focused on antifungal capacities of amphibian skin-produced antimicrobial peptides[6, 7]; commensal antifungal products[7, 8, 9]; antifungal properties of mucus[9], alkaloids[10], and lysozymes[11, 12] as well as the roles of antibodies[4,13]. Many of these studies suggest that *Bd* exposure can elicit some immune protection[14]. However, the contribution of skin-resident immune cells to amphibian anti-*Bd* defenses remains almost entirely unexplored.

Mammalian mast cells serve as sentinels of mucosal and connective tissues, concentrated in barrier tissues like skin, where they maintain homeostasis and regulate immune responses[15]. Other granulocyte-lineage cells such as neutrophils are generally not found in healthy tissues and only extravasate into sites of inflammation[16]. Consequently, mast cells are among the first immune cells to recognize and respond to skin-infiltrating pathogens. When activated, mast cells release pre-formed and *de novo*-generated immunomodulatory compounds that may serve to elicit, exacerbate, or ameliorate inflammatory responses[15]. Cells bearing hallmark mast cell cytology have been reported across a range of non-mammalian species[17, 18], including amphibians[19]. Notably, the principal mast cell growth factor, stem cell factor (SCF, KIT ligand) required for mast cell differentiation and survival[20] is expressed by all vertebrates examined to-date.

Here, we combine comprehensive *in vitro* and *in vivo* approaches to define the roles of amphibian (*Xenopus laevis*) mast cells during *Bd* infections. Our results provide compelling evidence that skin-resident immune cells contribute to anti-*Bd* defenses.

Results

Frog mast cells possess archetypal mast cell cytology and transcriptional profiles

We produced *X. laevis* recombinant (r)SCF, and used this reagent to generate mast cell cultures from bone marrow-derived myeloid precursors[21]. Mast cells were compared to bone marrow-derived neutrophilic granulocytes (hereafter referred to as 'neutrophils'), differentiated using a recombinant *X. laevis* colony-stimulating factor-3[21] (rCSF3, *i.e.*, granulocyte colony-stimulating factor; GCSF). While the neutrophil cultures were comprised of cells with hyper-segmented nuclei and neutral-staining cytoplasms (**Fig. 1A**), the mast cell cultures consisted predominantly of mononuclear cells with basophilic cytoplasm (**Fig. 1B**). We confirmed the granulocyte-lineage of *X. laevis* mast cells using specific esterase (SE) staining (**Fig. 1D**). As expected, *X. laevis* neutrophils were also SE-positive (**Fig. 1C**). Mast cell and neutrophil morphology was further explored with electron microscopy (**Fig. 1E-H**). SEM imaging demonstrated that *X. laevis* mast cells possess extensive folding of their plasma membranes (**Fig. 1F**). This mast cell-characteristic membrane ruffling appeared as projections resembling pseudopods via TEM, which further revealed electron-dense heterogenous granules, few mitochondria, and round to elongated nuclei (**Fig. 1H**) typical of mammalian mast cells[22]. *X. laevis* neutrophils also exhibited pronounced membrane ruffling (**Fig. 1E**) but strikingly distinct intracellular appearance including multilobed nuclei (**Fig. 1G**).

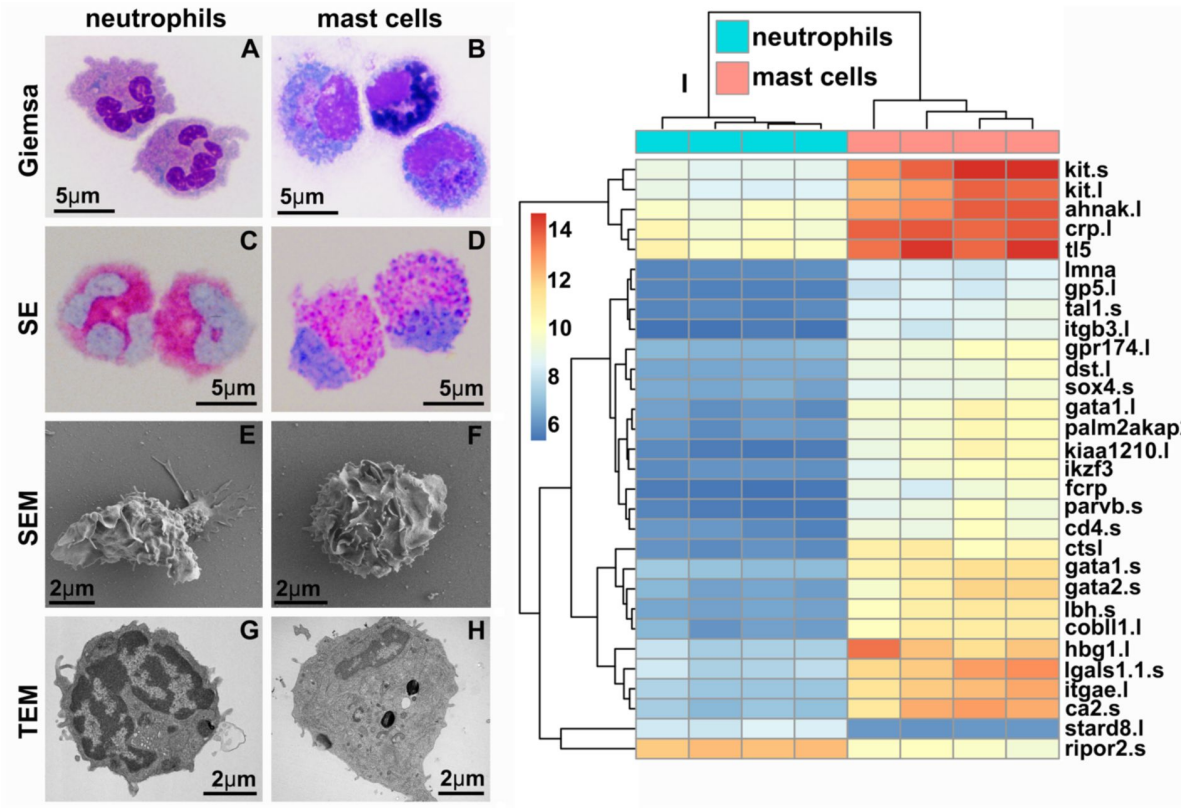

Figure 1.

X. laevis bone marrow-derived mast cells possess classical mast cell cytology and transcriptional profiles.

Neutrophils (**A**, **C**, **E**, **G**) and mast cells (**B**, **D**, **F**, **H**) were stained with Giemsa (**A**, **B**) and Leder to visualize specific esterase activity (SE) (**C**, **D**) or imaged with scanning and transmission electron microscopy (SEM: **E**, **F** and TEM: **G**, **H**). (**I**) Heat map of the top 30 differentially expressed genes (DEGs) identified with RNA sequencing analyses of *X. laevis* mast cell (*N*=4) and neutrophil (*N*=4) cultures. Log2fold change in expression represented as color scale.

Frog mast cells and neutrophils also exhibited distinct transcriptional profiles of immune- related genes including those encoding lineage-specific transcription factors, immune receptors, downstream signaling components and adhesion molecules, as well as non-immune genes (**Fig. 1I**). Frog mast cells and neutrophils each expressed greater levels of lineage-specific transcription factors associated with mammalian mast cell (gata1, gata2, and mitf)[23] and neutrophil (cebp family members)[24] counterparts, respectively (**Fig. 2A**). Notably, mast cells expressed greater levels of enzyme and cytokine genes associated with tissue remodeling (carboxypeptidase; cpa[25]), immune suppression (indoleamine 2,3 dioxygenase-1; ido1[26]) and amelioration of cutaneous inflammation (leukemia inhibitory factor, lif[27]; **Fig. 2B**). Conversely, neutrophils expressed predominantly proinflammatory enzymes and cytokine genes such as leukotriene 4 hydrolase (lta4h; **Fig. 2B**) and tumor necrosis factor alpha (tnfα, **Fig. 2B**). In addition, mast cells and neutrophils each had greater expression of genes encoding their respective growth factor receptors, kit and csf3r (**Fig. 2B**).

Enriching mast cells in frog skin offers protection against *Bd*

Although all granulocyte-lineage cells possess SE activity, mast cells are the predominant mononuclear granulocytes to reside in vertebrate tissues[28]. Therefore, we selectively enriched mast cells in *X. laevis* skin via subcutaneous rSCF administration (note SE-stained cells indicated by arrows in r-ctrl-injected skins, **Fig. 3A**, versus r-SCF-injected skins, **Fig 3B**). We confirmed SE- positive cells in rSCF-treated skins also possessed round-oval nuclei (**Fig. 3C**). Maximum mast cell enrichment was observed 12 hours post injection (hpi) of rSCF (**Fig. 3D**). When we challenged *X. laevis* with *Bd*, we did not detect differences in skin fungal loads between control (r-ctrl- injected) and mast cell-enriched groups at 7 days post infection (dpi; **Fig. 3E**). However, fungal loads were almost two-fold lower in mast cell- compared to control-enriched animals at 21 dpi, allowing for approximately four cycles of zoospore to mature zoosporangia development (**Fig. 3E**).

Mast cells protect frogs from *Bd*-elicited inflammation-associated pathology

To explore potential mechanisms of mast cell-mediated protection against *Bd,* we compared the gene expression profiles of r-ctrl- and rSCF-administered *Bd*-infected frog skins at 21 dpi. Among the top differentially expressed genes, we noted mast cell-enriched, *Bd*-infected skins possessed greater transcripts for genes associated with cutaneous strength and integrity (lamc2), epidermal cell maturation, lymphocyte recruitment (b3gnt3.1)[29, 30, 31], as well as ion and nutrient flow (gjb3l). (**Fig. 4A**). Moreover, mast cell-enriched *Bd*-challenged skin exhibited greater expression of genes associated with protection of the mucosa and epithelial healing (ttf3.6s)[32], pathogen nutrient deprivation in mucus (slc1a5s)[33], and mucus production (duoxa1.s[34]; **Fig. 4A**). In striking contrast, skins from control *Bd*-infected frogs revealed greater expression of genes associated with leukocyte infiltration and inflammation (*e.g.*, ccl19, cxcl16, adamt13, csf3r; **Fig. 4A**). These transcriptional profiles were supported by our histological observations wherein control *Bd*- infected skins exhibited hyperkeratosis, epidermal hyperplasia, jagged stratum corneum, and extensive leukocyte infiltration (**Fig. 4B**), while mast cell-enriched *Bd*-infected tissues appeared largely devoid of these pathologies (**Fig. 4C**).

Cutaneous neutrophil enrichment results in increased *Bd* fungal loads

Neutrophils are one of the first leukocytes to infiltrate infected tissues, typically amplifying inflammation[35]. All vertebrate neutrophils depend on CSF3 for their differentiation and function[36], and our previous work has demonstrated the gene encoding the CSF3 receptor

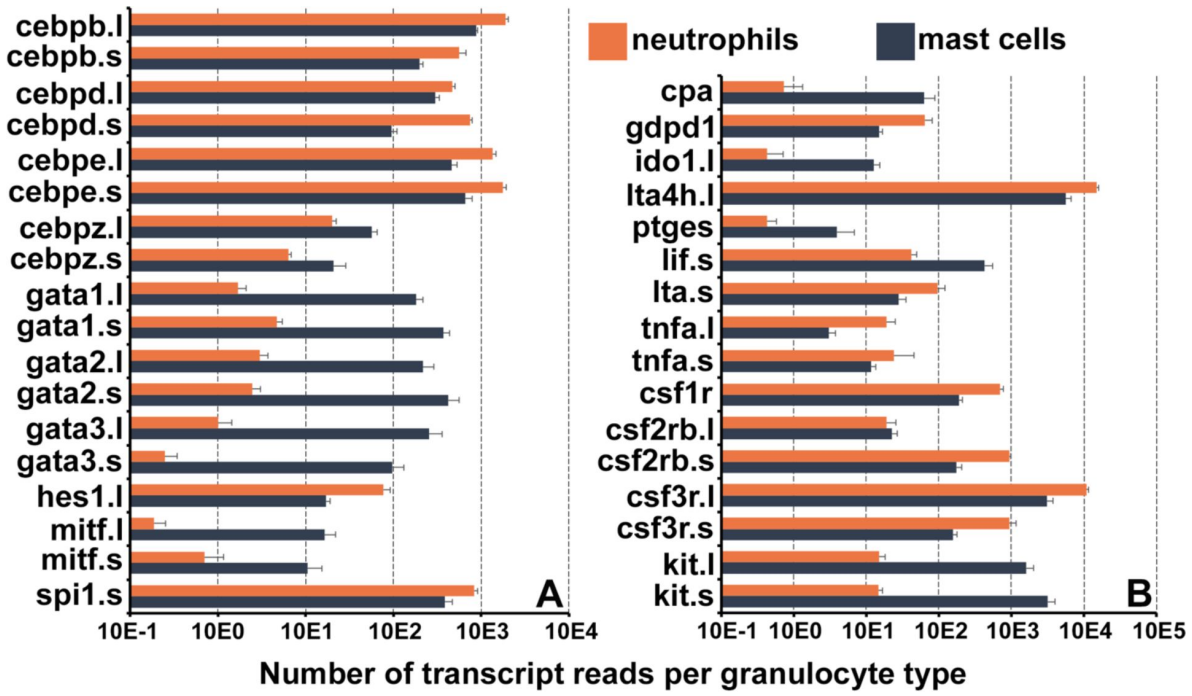

Figure 2.

Frog mast cells and neutrophils possess gene profiles similar to their mammalian counterparts.

The differentially expressed genes from the RNA sequencing analyses of *X. laevis* mast cells and neutrophil cultures were profiled for those encoding (**A**) transcription factors associated with mast cell- or neutrophil-specific lineages and (**B**) granulocyte antimicrobial components and growth factor receptor genes. All depicted genes were significantly differentially expressed between the two populations, *N*=4 per group.

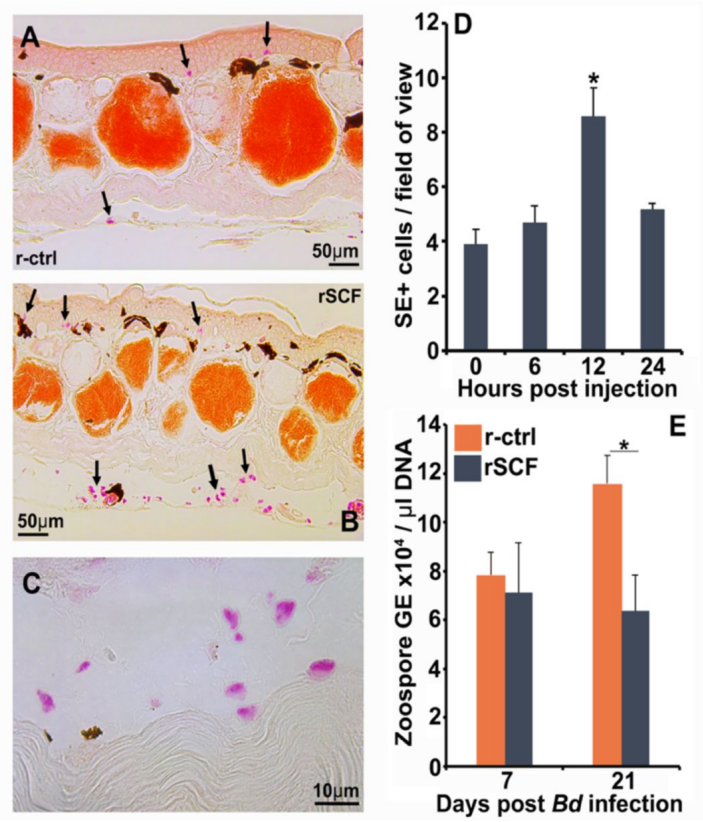

Figure. 3.

Enriching frog cutaneous mast cells lowers *Bd* loads.

Representative images of SE stained (**A**) control and (**B**) mast cell-enriched skin 12 hpi. (**C**) We confirmed the enriched population was composed of mono-morphonuclear cells. (**D**) Mast cell enrichment was optimized across several time points by quantifying SE-positive cells per field of view under 40x magnification. Results represent means ± SEM from 3 animals per time point (2 experimental repeats). (**E**) Mast cell-enriched and control dorsal skins were collected from *X. laevis* 7- and 21-dpi. *Bd* loads are represented as the number of zoospore genomic equivalents (GE) x 10^4 per μl of total input DNA. Time points were analyzed independently. Results represent means ± SEM from 7 animals per experimental group (*N*=7). Asterisks indicate significance: $p < 0.05$ by (**D**) one-way ANOVA with Tukey post-hoc analysis or (**E**) Student's t-test.

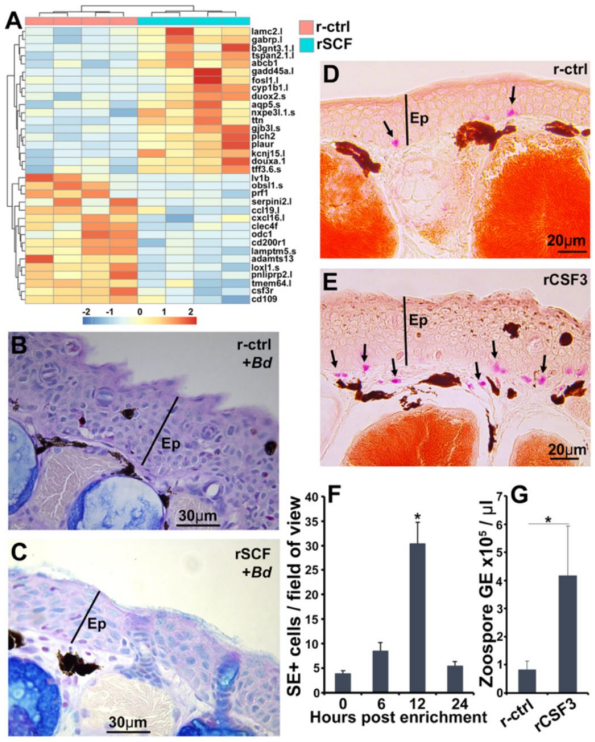

Figure. 4.

Consequences of cutaneous mast cell and neutrophil enrichment.

(**A**) RNAseq analysis of skin tissue from control (r-ctrl) or mast cell-enriched (rSCF) *Bd*-infected *X. laevis* at 21 dpi. Heat map of the top 30 DEGs, numbers matched to colors represent $\log^2$ fold change in expression. (**B** & **C**) Representative images of control and mast cell-enriched, *Bd*-infected skins, 21 dpi, demonstrating differences in epidermal thickening. (**D** & **E**) Representative images of control (r-ctrl) and neutrophil-enriched (rCSF3) skins collected 12 hpi demonstrating differences in epidermal thickening. (**F**) Kinetics of neutrophil enrichment following subcutaneous rCSF3 administration. Results are means ± SEM of SE-positive cells per field of view from 4 animals per time point (*N*=4). (**G**) *Bd* loads from control and neutrophil-enriched skin tissue 7 dpi, (*N*=6). Asterisks indicate significance: $p < 0.05$ by (**F**) one-way ANOVA with Tukey post-hoc analysis or (**G**) Student's t-test.

(csf3r) is a marker of *X. laevis* neutrophils[37], [38]. Because csf3r expression was markedly elevated in control over mast cell-enriched skins of infected frogs (**Fig. 4A**), we next assessed the outcomes of enriching skin for neutrophils via subcutaneous rCSF3 administration. We confirmed neutrophil enrichment peaked 12 hp rCSF3 injection (**Fig. 4F**) and resulted in a thickened epidermis in comparison with r-ctrl injected skins of otherwise healthy animals (*i.e.*, no *Bd*; **Fig. 4D, E**). When challenged with *Bd*, frogs with neutrophil-enriched skin possessed significantly greater *Bd* loads than control frogs (**Fig. 4G**). This suggests inflammation may be exacerbating *Bd* infections.

In vitro analyses of frog mast cells responses to *Bd*

Amphibians rely heavily on skin-produced antimicrobial peptides (AMPs) for antifungal protection[39], and mast cells produce antimicrobial AMPs[40]. Thus, we examined whether mast cells could be sources of such AMPs during *Bd* infections. As anticipated, mast cells, but not neutrophils challenged with *Bd*, upregulated their expression of the AMP-encoding genes, *pgla* and *magainin* (**Fig. S1A**).

Mammalian mast cells are recognized as potent producers of the pleotropic anti- inflammatory cytokine, interleukin-4 (IL4)[41]. Notably, *X. laevis* mast cells challenged *in vitro* with *Bd* significantly upregulated their il4 gene expression (**Fig. S1A**), whereas almost no il4 expression was detected from either unstimulated or *Bd*-challenged neutrophils. To examine whether the frog IL4 might offer anti-*Bd* protection, we generated the *X. laevis* IL4 in recombinant form (rIL4) and confirmed subcutaneous injection of this moiety augmented expression of genes typically activated by the mammalian IL4[42] (cd36, metalloproteinase inhibitor 3-timp3, and monoamine oxidase A- maoa; **Fig. S1B**). However, subcutaneous administration of rIL4 in *Bd*-infected frogs did not alter their fungal loads (**Fig. S1C**), suggesting IL4 is probably not a major mechanism responsible for the observed mast cell-mediated anti-*Bd* protection.

Enrichment of frog skin mast cells alters mucus gland composition

Because mast cell-enriched frog skin had greater expression of genes associated with mucosal tissue integrity and mucus production (**Fig. 4A**), we next investigated whether the anti-*Bd* protection identified in mast cell-enriched skins could be due, at least in part, to differences in mucus production. Interestingly, while mucus glands in mock- and *Bd*-infected control skin sections contained normal levels of mucus, those from both mock- and *Bd*-infected frogs that had been enriched for cutaneous mast cells were significantly more filled with higher levels of mucin (**Fig. 5A-C**).

Enrichment of frog skin mast cells alters skin microbial composition

Amphibian skin-produced mucus may offer antimicrobial protection and serve as a selective substratum for commensal microbes, many of which are antifungal[9]. We found no significant differences in direct *Bd*-killing capacities of mucus isolated from mock- or *Bd*-challenged control or mast cell-enriched frogs (**Fig. S2**). By contrast, we observed substantial differences in skin microbiomes, including changes in bacterial composition and richness as well as relative abundances of *Bd*-inhibitory bacteria (**Fig. 5D-G**, **Fig. S3**). A total of 1645 bacterial amplicon sequence variants (ASVs) were identified from 20 bacterial phyla, seven of which were predominant (**Fig. 5D**). Of these, *Verrucomicrobiota* were only present on uninfected animals, whereas *Acidobacteriota* was only seen after 21 dpi on both control and mast cell-enriched, infected animals (**Fig. 5D**).

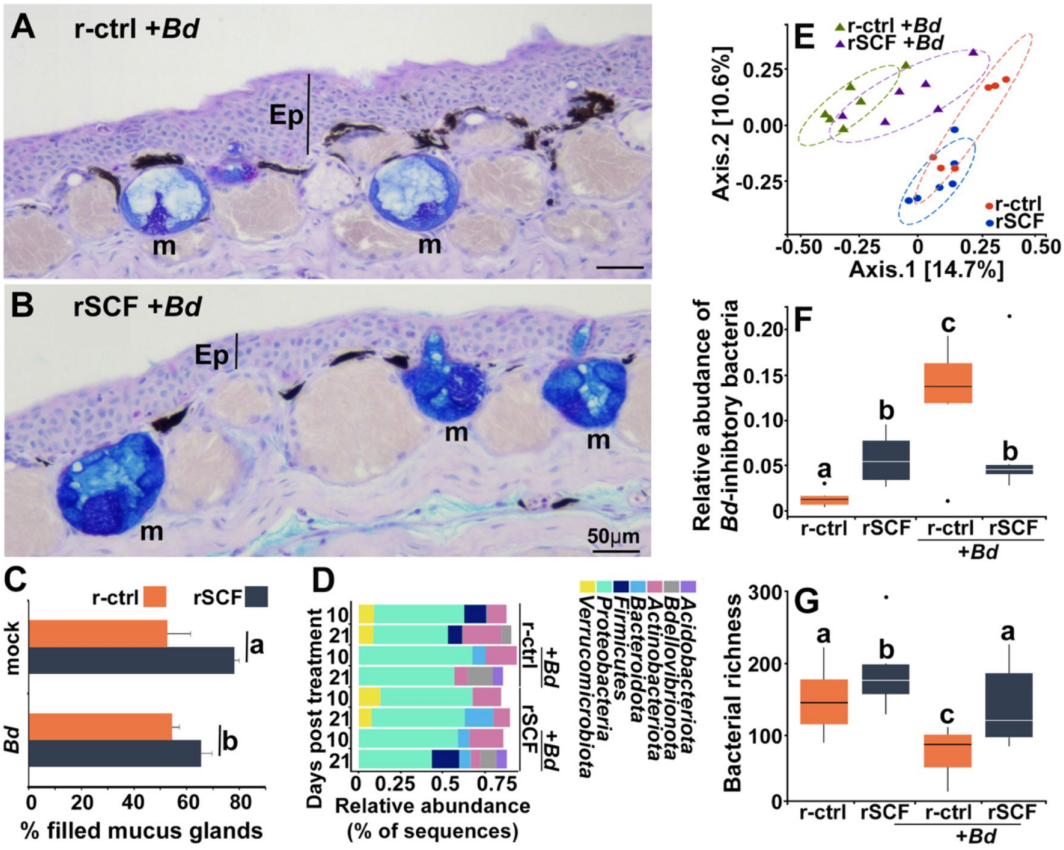

Figure. 5.

Cutaneous mast cells promote filled mucus glands.

Control (r-ctrl-injected) or mast cell-enriched (rSCF-injected) *X. laevis* were mock-infected or challenged with *Bd* for 21 days. Mucin content was examined in cutaneous mucus glands with Alcian Blue/PAS stain. Representative images of *Bd*-infected (**A**) control and (**B**) mast cell-enriched animals. Mucus glands are denoted by 'm', and epithelia are denoted by 'Ep'. (**C**) ImageJ software was used to determine the proportion of positive mucin staining within each mucus gland. Results are mean ± SEM percent positive mucin staining per mucus gland. Letters indicate group mean significance: $p < 0.05$ for treatment effects and interaction by two-way ANOVA. Skin tissue pieces from six individual frogs were used per treatment group (N=6). (**D**) Microbial phyla distribution across groups. Low abundance phyla (< 5% relative abundance are not shown). 10 dpi (**E**) community composition (Jaccard distances shown with 80% confidence ellipses) differed among all treatments. (**F**) Relative abundance of *Bd*-inhibitory bacteria and (**G**) bacterial richness were examined in control and mast cell enriched frogs, 10 days post *Bd* or mock challenge. Letters above bars in C, F and G indicate statistically different groups.

At 10 dpi, mast cell-enrichment resulted in a nominal shift in community composition compared to control frogs (**Fig. 5E**). Notably, while control, *Bd*-infected animals exhibited a drastic shift in community composition, mast cell-enriched animals possessed substantially less deviated community composition (**Fig. 5E**), suggesting that these cells are somehow counteracting the adverse effects of *Bd* on microbiome structure. These mast cell-mediated effects persisted to 21 dpi (**Fig. S3A**).

At 10 dpi, mast cell-enriched and mock-infected frogs possessed significantly greater abundance of *Bd*-inhibitory bacteria such as *Chyrseobacterium sp*., compared to control, mock infected animals (**Fig. 5F**)[43]. This suggests that mast cells may promote skin flora composition that is more antifungal. Control (non-enriched) *Bd*-infected frogs possessed significantly greater abundance of *Bd*-inhibitory bacteria than all other treatment groups (**Fig. 5F**). While mast cell- enriched, *Bd*-infected frogs had lower abundance of *Bd*-inhibitory bacteria than control infected frogs, they possessed higher abundance of inhibitory taxa than uninfected control animals (**Fig. 5F**). The *Bd*-inhibitory bacteria seen in greater abundance on mast cell-enriched, *Bd*-infected animals, included *Roseateles sp*., *Flavobacterium sp*., and *Kaistia sp*. We did not see significant differences in *Bd*-inhibitory bacteria across the treatment groups at 21 dpi (**Fig. S3B**).

Mast cell-enriched uninfected frogs exhibited increased frog skin bacterial richness at 10 dpi (**Fig. 5G**). While control *Bd*-infected animals exhibited significantly reduced skin microbial richness, mast cell-enriched *Bd*-infected frogs did not exhibit such a reduction in bacterial richness (**Fig. 5G**), supporting the idea that mast cells may be counteracting the adverse effects of *Bd* on skin microbiome composition.

Discussion

Amphibian extinction rates far outpace those of any other vertebrate class[44]. It is now well-established that chytrid fungi are major contributors to these declines, and strikingly, are considered the greatest infectious disease threat to biodivsersity[45]. The development of effective mitigation strategies though, is hindered by incomplete understanding of amphibian immune defenses and skin integrity. In this respect, while mast cells are recognized as key immune sentinels of tissues such as skin[46], relatively little is known about this cell lineage outside of mammals. Our findings provide the first in-depth functional analyses of these cells in amphibians and explore their protective mechanisms during chytrid infections. This work presents a unique perspective on the evolution of mast cell functionality and will serve as a new avenue to explore ways to counteract the amphibian declines.

Mammalian mast cells directly interact with neurons innervating the skin[47], and mucus production in mammals is tightly controlled by neuronal signaling[48]. In turn, mucus serves as a critical substratum for microbiota at mucosal barriers[49]. Here, we demonstrate that frog skin mast cells appear to confer significant protection against *Bd* by counteracting *Bd*-elicited inflammation, maintaining skin integrity, promoting mucus production, and preventing the disassembly of established skin microbiomes. Amphibian skin is much thinner and more permeable than that of mammals[7], and as such, arguably represents a more penetrable barrier to pathogens. Because mammalian skin is relatively impermeable, mast cells are absent from mammalian epidermis and are instead found exclusively in their dermal layers[50]. In contrast, we have shown here and have observed across several classes of amphibians[16] that mast cells are found in both epidermal and dermal layers. This localization has presumably evolved to support the more intimate contact between amphibian skin and their environments. Considering the importance of amphibian cutaneous integrity to their physiology[51], it is likely that skin-resident mast cells co-evolved to support skin immunity, physiology, and symbiotic microbiota.

Ongoing research continues to reveal functional differences between mammalian connective tissue and mucosa-resident mast cells[52], and we suspect that there is similarly much to learn about the distinct physiological and immune roles of amphibian epidermal and dermal mast cells.

Bd infections caused major reductions in bacterial taxa richness, changes in composition and substantial increases in the relative abundance of *Bd*-inhibitory bacteria early in the infection. Similar changes to microbiome structure occur during experimental *Bd* infections of red-backed salamanders and mountain yellow-legged frogs[8, 53]. In turn, progressing *Bd* infections corresponded with a return to baseline levels of *Bd*-inhibitory bacteria abundance and rebounding microbial richness, albeit with dissimilar communities to those seen in control animals. These temporal changes indicate that amphibian microbiomes are dynamic, as are the effects of *Bd* infections on them. Indeed, *Bd* infections may have long-lasting impacts on amphibian microbiomes[8]. While *Bd* infections manifested in these considerable changes to frog skin microbiome structure, mast cell enrichment appeared to counteract these deleterious effects to their microbial composition. Presumably, the greater skin mucosal integrity and mucus production observed after mast cell enrichment served to stabilize the cutaneous environment during *Bd* infections, thereby ameliorating the *Bd*-mediated microbiome changes. While this work explored the changes in established antifungal flora, we anticipate the mast cell-mediated inhibition of *Bd* may be due to additional, yet unidentified bacterial or fungal taxa. Intriguingly, while mammalian skin mast cell functionality depends on microbiome elicited SCF production by keratinocytes[54], our results indicate that frog skin mast cells in turn impact skin microbiome structure and likely their function. It will be interesting to further explore the interdependent nature of amphibian skin microbiomes and resident mast cells.

In contract to the mast cell effects, enrichment of neutrophils seemed to result in greater *Bd* skin burdens. This suggests that neutrophils and the cytokines they release may result in a greater level of inflammation, which is not protective. This is consistent with other studies that suggest that a strong immune response in the skin compartment of some species may be detrimental[55, 56]

It has become apparent that amphibian host-*Bd* interactions are highly complex and multifaceted while different amphibian species exhibit marked differences in their susceptibilities to this devastating pathogen[2, 4]. The findings described here emphasize the importance of skin-resident mast cells for successful anti-*Bd* defenses and demonstrate that these immune sentinels are intimately linked to many aspects of frog skin physiology. Our results indicate that when mast cells are enriched, the ensuing changes in the skin allow for greater resistance to infection by developing zoospores. Presumably, distinct amphibian species have evolved disparate interconnections between their skin mast cells and their cutaneous defenses, as dictated by their respective physiological and environmental pressures. In turn, these species-specific differences likely dictate whether and to what extent the skin-resident mast cells of a given amphibian species recognize and appropriately respond to *Bd* infections. We postulate that such differences may contribute to the differences in susceptibilities of amphibian species to pathogens like chytrid fungi.

Methods

Animals

Outbred 1 year-old (1.5-2”), mixed sex *X. laevis* were purchased from Xenopus 1 (Dexter, MI). All animals were housed and handled under strict laboratory regulations as per GWU IACUC (Approval number 15-024).

Recombinant cytokines and bone marrow granulocyte cultures

The *X. laevis* rSCF, rCSF3 and rIL4 were generated as previously described for rCSF3[57] and as detailed in the supplemental materials.

Bone marrow isolation, culture conditions, and establishment of neutrophil cultures have been previously described[58]. Mast cell cultures were generated according to protocols adapted from Koubourli et al. (2018) and Meurer et al. (2016) [59], [60]. Isolated bone marrow cells were treated with 250 ng/µl of rSCF on Day 0, Day 4, Day 7, and collected for further analysis on Day 9. Cell cultures were maintained at 27°C with 5% CO2 in amphibian medium supplemented with 10% fetal bovine serum and 0.25% *X. laevis* serum. Neutrophil-like granulocytes were generated as above but with 250 ng/µl of rCSF3 on Day 0, Day 3, and collected for further analysis on Day 5. Cell cultures were maintained at 27°C with 5% CO2 in amphibian serum-free medium supplemented with 10% fetal bovine serum, 0.25% *X. laevis* serum, 10 µg/mL gentamicin (Thermo Fisher Scientific, Waltham, Massachusetts, USA), 100 U/mL penicillin, and 100 µg/mL streptomycin (Gibco, Thermo Fisher Scientific).

Enrichment of skin granulocyte subsets

Animals were subcutaneously injected between the skin and muscle layers with 5 µg/animal of rSCF, rCSF3, or r-ctrl in 5 µL of saline using finely pulled glass needles. Optimal time course and dose for *in vivo* mast cell and neutrophil enrichment were determined during preliminary experiments.

Recombinant interleukin-4 treatment

The capacity of the recombinant interleukin-4 (rIL4) to induce expression of genes associated with mammalian IL4 responses were assessed by injecting frogs (*N*=6 per treatment group subcutaneously with rIL4 (5 µg/animal) or r-ctrl in 5 µl of saline. After 6hrs, animals were sacrificed, and skins were isolated for gene expression analyses.

To examine the effect of rIL4 on *Bd* loads, frogs were infected with *Bd* by water bath (10^5 zoospores/mL) as described below and 1 day later injected subcutaneously, dorsally with rIL4 (5 µg/animal) or r-ctrl in 5 µl of saline. After an additional 9 days of infection, animals were sacrificed and their dorsal skin *Bd* loads examined.

Bd stocks and fungal challenge

Bd isolate JEL 197 was grown in 1% tryptone broth or on 1% tryptone agar plates (Difco Laboratories, Detroit, MI) supplemented with 100 U/mL penicillin and 100 µg/mL streptomycin (Gibco) at 19°C.

In vitro Bd killing was evaluated by incubating live *Bd* (maturing zoosporangia) with mast cells or neutrophils at ratios of 5:1 or 1:1 *Bd* cells per granulocyte. Cells were incubated at 27°C for three days before fungal loads were analyzed by absolute qPCR. Experimental groups were compared to pathogen DNA amounts derived from equal quantities of live *Bd* plated alone in otherwise identical conditions.

For *in vivo* infection studies, zoospores were harvested by flooding confluent tryptone agar plates with 2 mL sterile A-PBS for 10 minutes. Twelve hours post rSCF, rCSF3, rIL4, or r-ctrl injection, animals were infected with 10^7 zoospores or mock-infected in 100 mL of water (10^5 zoospores/mL). After 3 hrs, 400 mL of water was added to each tank. Skins were collected for histology and gene expression analysis on 1, 7, and 21 dpi.

Histology

X. laevis leukocyte cytology and cutaneous SE staining has been described[57] and is detailed in the supplemental materials. An Alcian Blue/PAS staining kit (Newcomer Supply, Middleton, WI) was used to quantify mucin content from *in vivo* experiments. Histological analyses are detailed in the supplemental materials.

Electron Microscopy

Processing and imaging of cells for transmission and scanning electron microscopy (TEM and SEM) was conducted at the GWU Nanofabrication and Imaging Center (GWNIC). For transmission electron microscopy, cells were fixed as monolayers on six-well plates with 2.5% glutaraldehyde and 1% paraformaldehyde in 0.1 M sodium cacodylate buffer for one hour. Cells were treated with 1% osmium tetroxide in 0.1 M sodium cacodylate buffer for 1 hr. Following washes, cells were *en bloc* stained with 1% uranyl acetate in water overnight at 4°C. Samples were dehydrated through an ethanol series and embedded in epoxy resin using LX112. Inverted Beem capsules were placed into each tissue culture well to create *on face* blockfaces for sectioning. Resin was cured for 48 hrs at 60°C. The 95 nm sections were post-stained with 1% aqueous uranyl acetate and Reynold's lead citrate. All imaging was performed at 80 KV in a Talos 200X transmission electron microscope (Thermo Fisher Scientific, Hillsboro, OR).

For SEM, cells were fixed with 2.5% glutaraldehyde / 1% paraformaldehyde in Sodium cacodylate buffer, followed by 1% OsO4, then dehydrated through an ethyl alcohol series. Coverslips were critical point dried and coated with 2 nm iridium. Cells were imaged using a Teneo Scanning Electron Microscope (Thermo Fisher Scientific).

Analyses of immune gene expression and *Bd* skin loads

These analyses have been described[57] and are detailed in supplemental materials.

RNA sequencing

For transcriptomic profiling, bone marrow-derived neutrophil and mast cell cultures were generated as described above and FACS-sorted according to preestablished size and internal complexity parameters to isolate the respective subsets for further analyses. Sorted cells were immediately processed to extract and purify RNA. Flash frozen samples were sent to Azenta Life Sciences for all library preparation, RNA sequencing, and analyses. In short, polyadenylated RNA was isolated using Oligo dT beads. Enriched mRNAs were then fragmented for first and second strand cDNA synthesis. cDNA fragments were end repaired, 5' phosphorylated, and dA-tailed.

Fragments were then ligated to universal adaptors and PCR-amplified. 150-bp paired-end sequencing was performed on an Illumina HiSeq platform.

FastQC was used to evaluate raw data quality. Adaptors sequences and poor-quality nucleotides were removed from reads using Trimmomatic v.0.36. The STAR aligner v.2.55.2b was used to map these reads to the Xenopus_laevis_9_2 reference genome from ENSEMBL. To determine differential gene expression, featureCount (Subread package v.1.5.2) was first used to count unique gene hits, which were then used with DESeq2 to calculate absolute log2-fold change.

Skin microbiome analyses

Towards microbiome studies, frogs were housed individually (N=6/treatment group). At indicated times, frogs were gently rinsed with sterile deionized water to remove transient microbes and gently swabbed 20 times, dorsally. Genomic DNA was extracted from swabs using a PowerSoil Pro kit on a Qiacube HT (QIAGEN, MD). One-step PCR library prep and dual-index paired-end Illumina sequencing was used to sequence the skin microbiome of individual frogs. A ~380 base pair region

in the V3-V5 region of the 16S rRNA gene using the universal primers 515F-Y (GTGYCAGCMGCCGCGGTAA) and 939R (CTTGTGCGGGCCCCCGTCAATTC) was used for amplification. Negative and positive controls (ZymoBIOMICS D6300 & D6305, Zymo, CA) were included in each round of extraction and PCR. Reactions were done in duplicate for each sample, pooled, cleaned with in-house Speed-beads (in a PEG/NaCl buffer), quantified with a Qubit4 (Invitrogen, MA) and pooled into a final library in equimolar proportion. The pooled library was sequenced on two Illumina MiSeq runs (v3 chemistry: 2x300 bp kit) at the Center for Conservation Genomics, Smithsonian National Zoo & Conservation Biology Institute.

Analyses were performed in the R environment version 4.0.3 (R Core Team, 2020) using methods detailed in the supplemental materials.

Statistical analyses

Differences in transcript expression were calculated with one-way or multi-way ANOVAs followed by Tukey post-hoc tests. Student's t-tests were used to determine differences in *Bd* loads between treatments only. Statistical differences in mucin content and mucosome *Bd*-killing were assessed with the two-way ANOVA calculator available online through Statistics Kingdom. For RNA sequencing, *p*-values were calculated with the Wald test and were adjusted using the Benjamini-Hochberge procedure.

Acknowledgements

We thank Dr. Cynthia S. Dowd and Ben England (Chemistry Department, GWU) for their help with *X. laevis* mucus lyophilization. We thank Dr. Christine Brantner (GWU Nanofabrication and imaging center) for assistance with TEM and SEM imaging. KAH, MRHH, and AY were supported by Wilbur V. Harlan summer graduate research fellowships. KAH, MRHH, NR, NK, AY, MZ, and LG thank the GWU Biology Department.

Funding

National Science Foundation grant 2131061 (LG, CRMW) National Science Foundation grant 2147466 (LG, LAR-S) National Science Foundation grant 2147467 (LAR-S)

Author contributions

Conceptualization: KAH, LG

Methodology: KAH, MRHH, LKG, CNG, NR, NK, AY, MZ, EJJ, AND, LAR-S, CRMW, LG

Investigation: KAH, MRHH, LKG, CNG, NR, NK, AY, MZ, EJJ, AND, LAR-S, CRMW, LG

Visualization: KAH, MRHH, EJJ, AND, LG

Funding acquisition: LG, CRMW, LAR-S

Project administration: LG

Supervision: LG, CRMW, LAR-S

Writing – original draft: KAH, LAR-S, CRMW, LG

Writing – review & editing: KAH, LAR-S, CRMW, LG

Competing interests

The authors declare no competing interests.

Data and materials availability

All data are available in the main text or the supplementary materials.

Supplementary materials

Production of recombinant cytokines

The *X. laevis* SCF and CSF3 sequences representing the signal peptide-cleaved transcripts were ligated into the pMIB/V5 His A insect expression vectors (Invitrogen). SCF-ligated, CSF3-ligated, or empty vectors were transfected into Sf9 insect cells (cellfectin II, Invitrogen). Recombinant proteins contain a V5 epitope, and western blot with an anti-V5-HRP antibody (Sigma) confirmed their presence. Positive transfectants were selected using 10 µg/mL blasticidin (Gibco). Expression cultures were scaled up to 500 mL liquid cultures, grown for 5 days, pelleted by centrifugation, and the supernatants collected. Supernatants were dialyzed overnight at 4°C against 150 mM sodium phosphate, concentrated against polyethylene glycol flakes (8 kDa) at 4°C, dialyzed overnight at 4°C against 150 mM sodium phosphate, and passed through Ni-NTA agarose columns (Qiagen). Columns were washed with 2 × 10 volumes of high stringency wash buffer (0.5% Tween 20, 50 mM Sodium Phosphate, 500 mM Sodium Chloride, 100 mM Imidazole) and 5 x 10 volumes of low stringency wash buffer (as above but with 40 mM Imidazole). Recombinant proteins were eluted with 250 mM imidazole. After recombinant protein purification, a halt protease inhibitor cocktail (containing AEBSF, aprotinin, bestatin, E-64, leupeptin and pepstatin A; Thermo Scientific) was added. Intact recombinant protein presence was confirmed again by western blot and the protein concentrations quantified by Bradford protein assays (BioRad). Protein aliquots were stored at -20°C until use.

Bone marrow granulocyte cultures

Bone marrow cells were isolated as previously described [58]. Briefly, adult *X. laevis* (approximately one year old) were euthanized in 5% tricaine mesylate followed by cervical dislocation. Femurs were removed and washed in ice-cold Amphibian-PBS (A-PBS) in sterile conditions. Each femur was flushed with 5 mL of A-PBS. Red blood cells were removed from culture via a differential gradient generated with 51% Percoll. Bone marrow cell counts were generated using trypan blue exclusion and cells were seeded at a density of 10^4 cells/well for gene expression experiments, $5x10^4$ cells/well for histology analyses, and 10^5 cells/well for electron microscopy analyses.

Histology

Paraffin-embedded tissue sections (5 μm) were deparaffinized, rehydrated through A- PBS, and stained with Naphthol AS-D Chloroacetate (specific esterase; Sigma) or Alcian Blue/PAS (Newcomer, Middleton, WI) according to the manufacturers' instructions and optimized for *Xenopus* skin tissues. Cells collected from *in vitro* cultures were cytocentrifuged onto glass microscope slides (VWR). Cells were stained immediately with Giemsa (Sigma) for 7 minutes or fixed with 10% neutral buffered formalin for 30 minutes and stained with specific esterase according to the manufacturers' instructions. Slides stained with Alcian Blue/PAS (Newcomer) were used to quantify mucin content from *in vivo* experiments. Images were taken using identical microscope settings under 20x magnification. Images were converted to 8-bit in Fiji by ImageJ and threshold adjusted such that positive staining for mucus was captured within the mucus glands (threshold held constant across images). The percentage of each mucus gland positively stained and the average percent-positive per field of view were subsequently calculated. Positive staining of both acidic and neutral mucins was included in analyses. All slides were imaged with a Leica DMi8 Inverted Fluorescent Microscope with all mucus glands assessed for each respective frog skin section (Leica Microsystems, Davie, FL).

Analyses of immune gene expression and *Bd* skin loads

Cells and tissues were homogenized in Trizol reagent, flash frozen on dry ice, and stored at -80°C until RNA and DNA isolation. RNA isolation was performed using Trizol according to the manufacturer's directions. RNA-Seq is described in detail below. For qRT-PCR gene expression analysis, RNA (500 ng/sample) was reverse transcribed into cDNA using cDNA qscript supermix (Quantabio, Beverly, MA). Following RNA extraction, back extraction buffer (4 M guanidinethiocyanate, 50 mM sodium citrate, 1 M Tris pH 8.0) was mixed with the remaining Trizol layer and centrifuged to isolate the DNA-containing aqueous phase. DNA was precipitated overnight with isopropanol, pelleted by centrifugation, washed with 80% ethanol, and resuspended in TE buffer (10 mM Tris pH 8.0, 1 mM EDTA). DNA was purified by phenol:chloroform extraction and resuspended in molecular grade water (VWR).

Quantitative gene expression analyses for both *Bd* and *X. laevis* cells and tissues were performed using the CFX96 Real-Time System (Bio-Rad Laboratories, Hercules, CA) and iTaq Universal SYBR Green Supermix (Bio-Rad Laboratories). The Bio-Rad CFX Manager software (SDS) was employed for all expression analysis. All expression analyses were conducted using the ΔΔCt method relative to the *gapdh* endogenous control gene for *X. laevis.* Fungal load quantification was assessed by absolute qPCR. Isolated *Bd* DNA (JEL 197 isolate) was serially diluted and used as the standard curve. Primers were designed and validated against the *Bd* ribosomal RNA internal transcribed spacer 1 (ITS1). The primers used are listed in **Table S1**.

Analyses of mucus *Bd*-killing capacities

Mucosomes were collected from mast cell- or vector- enriched *X. laevis* that were either mock- or *Bd*-infected for 10 or 21 days. To this end, individual *X. laevis* were soaked in a 5 mL water bath for 1 hour. Each water sample was then lyophilized, reconstituted with 500 µl of molecular grade water, and passed through a sterile cell strainer to remove large debris.

Bd was seeded in opaque white 96-well plates (20,000 zoospores in 50 µl of tryptone broth / well). Next, 50 µl of mucosome solution was added to each well (100 µl total well volume) in three replicate wells per individual *X. laevis* mucosome. Mucosomes, tryptone broth, and water were each plated alone as controls. Plates were sealed with parafilm and incubated at 19°C for 16 hrs with gentle mixing (20 rpm).

Zoospore viability was determined with the CellTiter-Glo 2.0 Cell Viability assay kit (Promega) according to the manufacturer's instructions and using a SpectraMax plate reader (Molecular Devices, San Jose, CA). Luminescence readings were fitted to a standard curve (descending proportions of heat-killed zoospores to viable zoospores) to calculate the number of viable zoospores in each well. Zoospores were heated-killed at 65°C for 15 mins.

Skin microbiome analyses

All analyses were performed in the R environment version 4.0.3 (R Core Team, 2020). Demultiplexed reads were imported from Basespace into R environment for sequence processing. Package "dada2"[61] was used to perform quality filtering using their standard filtering parameters (*i.e.*, maxEE = 2), which collapsed high quality reads into amplicon sequence variant (ASV) and removed chimeras. Bacterial taxonomy was assigned using Silva version 138.1. The R package "phyloseq"[62] was used to import and merge the final ASV table, taxonomy table, and metadata to create a phyloseq object to perform further analyses. Sequences classified as cyanobacteria/chloroplast and those unclassified at kingdom were removed. Singletons were filtered out (*i.e.*, ASVs with only one sequence read in one individual). The R package "decontam"[63] was used to remove potential contaminants using the method "combined." The ZymoBIOMICS microbial community standards (positive controls) were analyzed, and we found genera in similar relative abundances as described by Zymo.

To determine how *Bd* and mast cell treatments impacted skin microbiomes, the microbiome structure was examined. The components of microbiome structure were: ASV richness (measured as *Bd*-inhibitory ASV richness and total ASV richness), microbial composition (measured by Jaccard and Bray-Curtis distances), and sequence abundance of *Bd*-inhibitory ASVs (measured as individual *Bd*-inhibitory ASV sequence counts and total relative abundance of *Bd*-inhibitory ASVs). To characterize variation in microbiome structure, Mast Cell (mast cell normal and mast cell+), *Bd* (*Bd*- and *Bd*+) and their interaction as explanatory variables at two-time points Day 10 and Day 21 post *Bd* infection were included. For this characterization, log-transformed ASV richness in ANOVAs, microbial composition measures in PERMANOVAs and log-transformed raw sequence counts in ANOVAs (with post-hoc corrections for multiple comparisons) were used. For identification of *Bd*-inhibitory ASVs, methods as described in by Jimenez *et al*., 2022[64] were followed.

Target Name	Primer Sequence (5'→ 3')
***Bd* its1 sense**	GCCATATGTCACGAGTCGAA
***Bd* its1 antisense**	GCCAAGAGATCCGTTGTCA
gapdh sense	GACACTCACTCCTCCATCTTTG
gapdh antisense	TGCTGTAGCCGCATTCATTA
hdc sense	GAATCTGAAAGCTGGGAGAGAA
hdc antisense	GATGTCAGGGCAGGAAAGTAG
il4 sense	GACATCAAGGACACCTGAAGAA
il4 antisense	GTCACAGGGAATCGGTACTAAAC
mag sense	GGCCTTTGCAGATGAAGATTTAG
mag antisense	CTACTGCTTCTGCATCTCGTT
pgla sense	CTGCACTCTGTGCAACCATAA
pgla antisense	CTCCAGCTTTAGATGCCATTCC

Table S1.

List of primer sequences

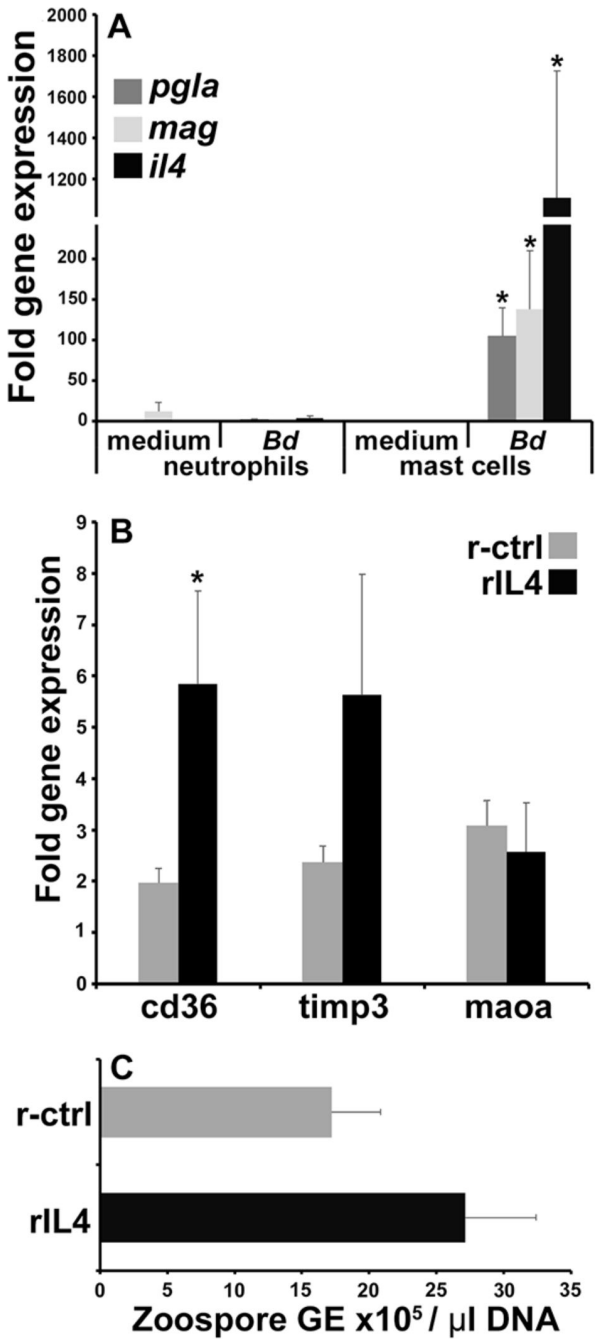

Figure. S1.

In vitro* analyses of frog mast cells and neutrophils challenged with *Bd (**A**) Mast cells and neutrophils derived from bone marrow of 6 individual frogs (*N*=6) were co- cultured with *Bd* (5 fungal cells per granulocyte) for 6 hrs prior to gene expression analyses of the antimicrobial peptide genes PGLa (*pgla*) and magainin (*mag*) or interleukin-4 (*il4*). (**B**) Changes in gene expression of selected genes in skin following subcutaneous injection of rIL4 (*N*=7). (**C**) Frogs were exposed to *Bd* and 24 hrs later injected subcutaneously with rIL4 or r-ctrl. Skin *Bd* loads were assessed 9 days following injection (*N*=8, per group). For B, asterisks denote statistically significant differences in expression following *Bd*-challenge compared to medium controls in mast cell cultures, one- way ANOVA with Tukey post-hoc analysis $p < 0.05$. For C, asterisk indicates significantly increased expression of cd36 by Student's t test, $p < 0.05$.

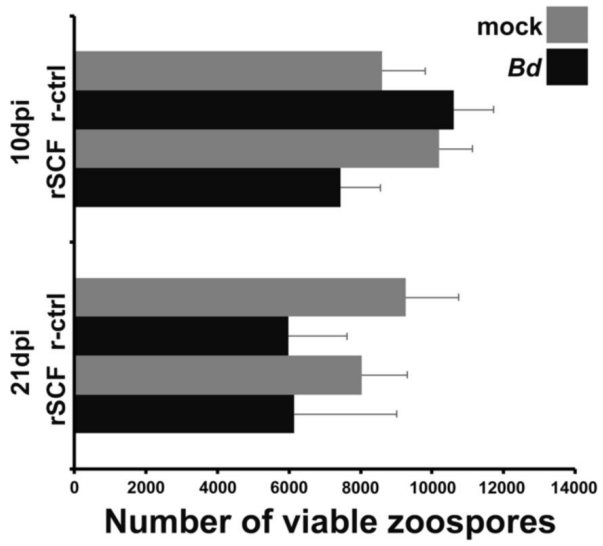

Figure. S2.

Mucosomes from mast cell-enriched frogs do not confer *Bd* killing.

Differences in musocome-killing capacities were determined by incubating zoospores with total mucosome contents for 16 hrs. Mucosomes were acquired from 10- or 21-day mock- or *Bd*-infected *X. laevis* that were injected with rSCF (mast cell-enriched) or r-ctrl (control). Results are mean ± SEM and were analyzed via a two-way ANOVA; 10- and 21-day experimental groups were analyzed independently; alpha set at 0.05. *N* = 5 experimental animals per treatment group for 10 dpi analyses and *N*= 8 experimental animals per treatment group for 21 dpi analyses.

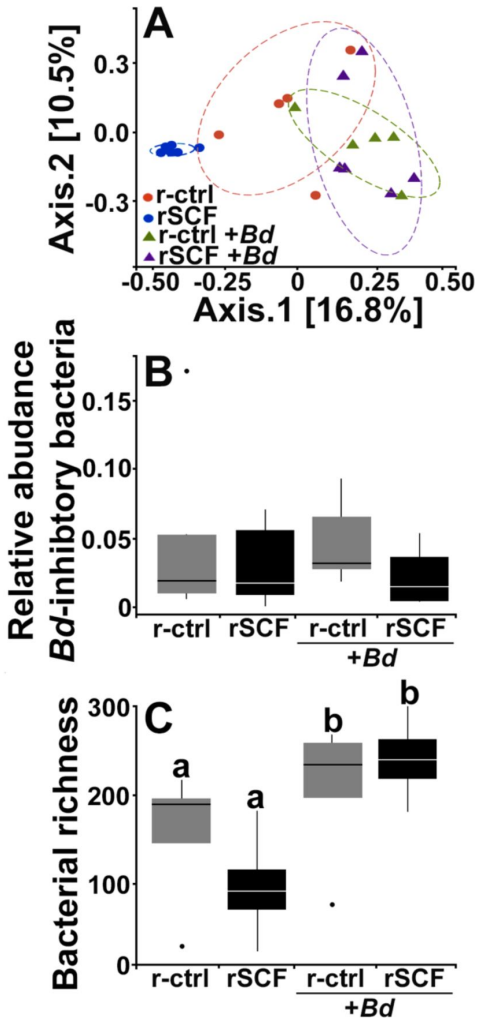

Figure. S3.

Mast cell enrichment protects frogs from *Bd*-mediated changes to skin microbiomes.

21 days post mock or *Bd*-challenge, we examined (**A**) community composition (Jaccard distances shown with 80% confidence ellipses), (**F**) relative abundance of *Bd*-inhibitory bacteria and (**G**) bacterial richness. Letters above bars indicate statistically distinct groups.

References

1. Martel A., et al. (2014) **Wildlife disease. Recent introduction of a chytrid fungus endangers Western Palearctic salamanders** *Science* **346**:630–631

2. Scheele B.C., et al. (2019) **Amphibian fungal panzootic causes catastrophic and ongoing loss of biodiversity** *Science* **363**:1459–1463

3. Van Rooij P., Martel A., Haesebrouck F., Pasmans F (2015) **Amphibian chytridiomycosis: a review with focus on fungus-host interactions** *Veterinary research* **46**:1–22

4. Van Rooij P., et al. (2010) **Development of in vitro models for a better understanding of the early pathogenesis of Batrachochytrium dendrobatidis infections in amphibians** *Altern Lab Anim* **38**:519–528

5. Voyles J., et al. (2009) **Pathogenesis of chytridiomycosis, a cause of catastrophic amphibian declines** *Science* **326**:582–585

6. Rollins-Smith L.A (2023) **The importance of antimicrobial peptides (AMPs) in amphibian skin defense** *Dev Comp Immunol* **142**

7. Varga J.F.A., Bui-Marinos M.P., Katzenback B.A (2018) **Frog Skin Innate Immune Defences: Sensing and Surviving Pathogens** *Front Immunol* **9**

8. Jani A.J., et al. (2021) **The amphibian microbiome exhibits poor resilience following pathogen-induced disturbance** *ISME J* **15**:1628–1640

9. Woodhams D.C., McCartney J., Walke J.B., Whetstone R (2023) **The adaptive microbiome hypothesis and immune interactions in amphibian mucus** *Dev Comp Immunol* **104690**

10. Rodriguez C., Rollins-Smith L., Ibanez R., Durant-Archibold A.A., Gutierrez M (2017) **Toxins and pharmacologically active compounds from species of the family Bufonidae (Amphibia Anura). J Ethnopharmacol** **198**:235–254

11. Grogan L.F., et al. (2018) **Review of the Amphibian Immune Response to Chytridiomycosis, and Future Directions** *Front Immunol* **9**

12. Rollins-Smith L.A., et al. (2009) **Immune defenses of Xenopus laevis against Batrachochytrium dendrobatidis** *Front Biosci (Schol Ed* **1**:68–91

13. Ramsey J.P., Reinert L.K., Harper L.K., Woodhams D.C., Rollins-Smith L.A (2010) **Immune defenses against Batrachochytrium dendrobatidis, a fungus linked to global amphibian declines, in the South African clawed frog, Xenopus laevis** *Infect Immun* **78**:3981–3992

14. McMahon T.A., et al. (2014) **Amphibians acquire resistance to live and dead fungus overcoming fungal immunosuppression** *Nature* **511**:224–227

15. Sobiepanek A., et al. (2022) **The multifaceted roles of mast cells in immune homeostasis, infections and cancers** *International Journal of Molecular Sciences* **23**

16. Hauser K.A., Garvey C.N., Popovic M., Grayfer L (2023) **Biology of amphibian granulocytes - From evolutionary pressures to functional consequences** *Dev Comp Immunol* **140**

17. McNeil H.P., Adachi R., Stevens R.L (2007) **Mast cell-restricted tryptases: structure and function in inflammation and pathogen defense** *Journal of Biological Chemistry* **282**:20785–20789

18. Abraham S.N., St John A.L (2010) **Mast cell-orchestrated immunity to pathogens** *Nature reviews.Immunology* **10**:440–452

19. Baccari G.C., Pinelli C., Santillo A., Minucci S., Rastogi R.K (2011) **Mast cells in nonmammalian vertebrates: an overview** *International review of cell and molecular biology* **290**:1–53

20. Ito T., et al. (2012) **Stem cell factor programs the mast cell activation phenotype** *J Immunol* **188**:5428–5437

21. Yaparla A., Wendel E.S., Grayfer L (2016) **The unique myelopoiesis strategy of the amphibian Xenopus laevis** *Developmental & Comparative Immunology* **63**:136–143

22. Espinosa-Riquer Z.P., et al. (2020) **Signal transduction pathways activated by innate immunity in mast cells: translating sensing of changes into specific responses** *Cells* **9**

23. Cildir G., et al. (2021) **Understanding mast cell heterogeneity at single cell resolution** *Trends in Immunology* **42**:523–535

24. Paudel S., Ghimire L., Jin L., Jeansonne D., Jeyaseelan S (2022) **Regulation of emergency granulopoiesis during infection** *Front Immunol* **13**

25. Atiakshin D., et al. (2022) **Carboxypeptidase A3-A Key Component of the Protease Phenotype of Mast Cells** *Cells* **11**

26. Baban B., et al. (2009) **IDO activates regulatory T cells and blocks their conversion into Th17-like T cells** *J Immunol* **183**:2475–2483

27. Banner L.R., Patterson P.H., Allchorne A., Poole S., Woolf C.J (1998) **Leukemia inhibitory factor is an anti- inflammatory and analgesic cytokine** *J Neurosci* **18**:5456–5462

28. Agis H., et al. (1996) **Mast Cell-Lineage Versus Basophil Lineage Involvement in Myeloproliferative and Myelodysplastic Syndromes: Diagnostic Role of Cell-Immunopheno typing** *Leukemia & lymphoma* **22**:187–204

29. Kiritsi D., Has C., Bruckner-Tuderman L (2013) **Laminin 332 in junctional epidermolysis bullosa** *Cell adhesion & migration* **7**:135–141

30. Chang E.H., Van Camp G., Smith R.J (2003) **The role of connexins in human disease** *Ear and hearing* **24**:314–323

31. Pereira M.S., et al. (2018) **Glycans as key checkpoints of T cell activity and function** *Frontiers in immunology* **9**

32. Taupin D., Podolsky D.K (2003) **Trefoil factors: initiators of mucosal healing** *Nat Rev Mol Cell Biol* **4**:721–732

33. Kandasamy P., Gyimesi G., Kanai Y., Hediger M.A (2018) **Amino acid transporters revisited: New views in health and disease** *Trends Biochem Sci* **43**:752–789

34. Fischer H (2009) **Mechanisms and function of DUOX in epithelia of the lung** *Antioxid Redox Signal* **11**:2453–2465

35. Wang J (2018) **Neutrophils in tissue injury and repair** *Cell Tissue Res* **371**:531–539

36. Roberts A.W (2005) **G-CSF: a key regulator of neutrophil production, but that's not all!** *Growth Factors* **23**:33–41

37. Koubourli V.D., Wendel E.S., Yaparla A., Ghaul J.R., Grayfer L (2017) **Immune roles of amphibian (Xenopus laevis) tadpole granulocytes during Frog Virus 3 ranavirus infections** *Dev Comp Immunol* **72**:112–118

38. Yaparla A., Wendel E.S., Grayfer L (2016) **The unique myelopoiesis strategy of the amphibian Xenopus laevis** *Dev Comp Immunol* **63**:136–143

39. Patocka J., Nepovimova E., Klimova B., Wu Q., Kuca K (2019) **Antimicrobial peptides: amphibian host defense peptides** *Current medicinal chemistry* **26**:5924–5946

40. Di Nardo A., Yamasaki K., Dorschner R.A., Lai Y., Gallo R.L (2008) **Mast cell cathelicidin antimicrobial peptide prevents invasive group A Streptococcus infection of the skin** *J Immunol* **180**:7565–7573

41. Babina M., Guhl S., Artuc M., Zuberbier T (2016) **IL-4 and human skin mast cells revisited: reinforcement of a pro-allergic phenotype upon prolonged exposure** *Archives of dermatological research* **308**:665–670

42. Bhattacharjee A., et al. (2013) **IL-4 and IL-13 employ discrete signaling pathways for target gene expression in alternatively activated monocytes/macrophages** *Free Radic Biol Med* **54**:1–16

43. Woodhams D.C., et al. (2015) **Antifungal isolates database to centralize data on amphibian ski associated bacteria and their function against emerging fungal pathogens including Batrachochytrium dendrobatidis** *Ecology* **96**

44. **https://www.iucnredlist.org/resources/summary-statistics, I.R.L.**

45. Fisher M.C., Garner T.W (2020) **Chytrid fungi and global amphibian declines** *Nature Reviews Microbiology* **18**:332–343

46. St. John A.L., Rathore A.P., Ginhoux F (2023) **New perspectives on the origins and heterogeneity of mast cells** *Nature Reviews Immunology* **23**:55–68

47. Zhang S., Sumpter T.L., Kaplan D.H (2022) **Neuron–Mast Cell Cross-Talk in the Skin** *J Invest Dermatol* **142**:841–848

48. Baraniuk J.N (2008) **Neural regulation of mucosal function** *Pulm Pharmacol Ther* **21**:442–448

49. Paone P., Cani P.D (2020) **Mucus barrier, mucins and gut microbiota: the expected slimy partners?** *Gut* **69**:2232–2243

50. Cowen T., Trigg P., Eady R.A (1979) **Distribution of mast cells in human dermis: development of a mapping technique** *Br J Dermatol* **100**:635–640

51. Larsen E.H (2021) **Dual skin functions in amphibian osmoregulation** *Comparative Biochemistry and Physiology Part A: Molecular & Integrative Physiology* **253**

52. West P.W., Bulfone-Paus S (2022) **Mast cell tissue heterogeneity and specificity of immune cell recruitment** *Front Immunol* **13**

53. Muletz-Wolz C.R., Fleischer R.C., Lips K.R (2019) **Fungal disease and temperature alter skin microbiome structure in an experimental salamander system** *Mol Ecol* **28**:2917–2931

54. Wang Z., et al. (2017) **Skin microbiome promotes mast cell maturation by triggering stem cell factor production in keratinocytes** *J Allergy Clin Immunol* **139**:1205–1216

55. Ellison A.R., et al. (2014) **More than skin deep: functional genomic basis for resistance to amphibian chytridiomycosis** *Genome Biol Evol* **7**:286–298

56. Savage A.E., Gratwicke B., Hope K., Bronikowski E., Fleischer R.C (2020) **Sustained immune activation is associated with susceptibility to the amphibian chytrid fungus** *Mol Ecol* **29**:2889–2903

57. Hauser K., et al. (2020) **Discovery of granulocyte-lineage cells in the skin of the amphibian Xenopus laevis** *FACETS* **5**

58. Yaparla A., Grayfer L (2018) **Isolation and culture of amphibian (Xenopus laevis) sub-capsular liver and bone marrow cells** *Xenopus: Methods and Protocols* :275–281

59. Koubourli D.V., Yaparla A., Popovic M., Grayfer L (2018) **Amphibian (Xenopus laevis) interleukin-8 (CXCL8): a perspective on the evolutionary divergence of granulocyte chemotaxis** *Frontiers in immunology* **2058**

60. Meurer S.K., et al. (2016) **Isolation of mature (peritoneum-derived) mast cells and immature (bone marrow- derived) mast cell precursors from mice** *PLoS One* **11**

61. Callahan B.J., et al. (2016) **DADA2: High-resolution sample inference from Illumina amplicon data** *Nat Methods* **13**:581–583

62. McMurdie P.J. (2013) **S. phyloseq: an R package for reproducible interactive analysis and graphics of microbiome census data** *PLoS One* **8**

63. Davis N.M., Proctor D.M., Holmes S.P., Relman D.A., Callahan B.J (2018) **Simple statistical identification and removal of contaminant sequences in marker-gene and metagenomics data** *Microbiome* **6**

64. Jimenez R.R., et al. (2022) **Inhibitory Bacterial Diversity and Mucosome Function Differentiate Susceptibility of Appalachian Salamanders to Chytrid Fungal Infection** *Appl Environ Microbiol* **88**

Article and author information

Kelsey A. Hauser
Department of Biological Sciences, The George Washington University, Washington, DC, USA

Muhammad R. H. Hossainey
Department of Biological Sciences, The George Washington University, Washington, DC, USA

Lindsey K. Gentry
Center for Conservation Genomics, Smithsonian National Zoo & Conservation Biology Institute, Washington, DC, USA

Christina N. Garvey
Department of Biological Sciences, The George Washington University, Washington, DC, USA

Netra Ranganathan
Department of Biological Sciences, The George Washington University, Washington, DC, USA

Amulya Yaparla
Department of Biological Sciences, The George Washington University, Washington, DC, USA

Namarta Kalia
Department of Biological Sciences, The George Washington University, Washington, DC, USA

Mira Zelle
Department of Biological Sciences, The George Washington University, Washington, DC, USA

Elizabeth J. Jones
Department of Oncology, Lombardi Comprehensive Cancer Center, Georgetown University, Washington DC, USA

Anju N. Duttargi
Department of Oncology, Lombardi Comprehensive Cancer Center, Georgetown University, Washington DC, USA

Louise A. Rollins-Smith
Departments of Pathology, Microbiology and Immunology, and of Pediatrics, Vanderbilt University School of Medicine, Nashville, TN, USA, Department of Biological Sciences, Vanderbilt University, Nashville, TN, USA

Carly R. Muletz-Wolz
Center for Conservation Genomics, Smithsonian National Zoo & Conservation Biology Institute, Washington, DC, USA

Leon Grayfer
Department of Biological Sciences, The George Washington University, Washington, DC, USA
For correspondence: leon_grayfer@gwu.edu

Copyright

Editors

Reviewing Editor
Brian Kim
Icahn School of Medicine at Mount Sinai, New York, United States of America

Senior Editor
Satyajit Rath
Indian Institute of Science Education and Research (IISER), Pune, India

Reviewer #1 (Public Review):

Summary:
The global decline of amphibians is primarily attributed to deadly disease outbreaks caused by the chytrid fungus, Batrachochytrium dendrobatidis (Bd). It is unclear whether and how skin-resident immune cells defend against Bd. Although it is well known that mammalian mast cells are crucial immune sentinels in the skin and play a pivotal role in the immune recognition of pathogens and orchestrating subsequent immune responses, the roles of amphibian mast cells during Bd infections are largely unknown. The current study developed a novel way to enrich X. laevis skin mast cells by injecting the skin with recombinant stem cell factor (SCF), a KIT ligand required for mast cell differentiation and survival. The investigators found an enrichment of skin mast cells provides X. laevis substantial protection against Bd and mitigates the inflammation-related skin damage resulting from Bd infection. Additionally, the augmentation of mast cells leads to increased mucin content within cutaneous mucus glands and shields frogs from the alterations to their skin microbiomes caused by Bd.

Strengths:
This study underscores the significance of amphibian skin-resident immune cells in defenses against Bd and introduces a novel approach to examining interactions between amphibian hosts and fungal pathogens.

Weaknesses:
The main weakness of the study is the lack of functional analysis of X. laevis mast cells. Upon activation, mast cells have the characteristic feature of degranulation to release histamine, serotonin, proteases, cytokines, and chemokines, etc. The study should determine whether X. laevis mast cells can be degranulated by two commonly used mast cell activators IgE and compound 48/80 for IgE-dependent and independent pathways. This can be easily done in vitro. It is also important to assess whether in vivo these mast cells are degranulated upon Bd infection using avidin staining to visualize vesicle releases from mast cells. Figure 3 only showed rSCF injection caused an increase in mast cells in naïve skin. They need to present whether Bd infection can induce mast cell increase and rSCF injection under Bd infection causes a mast cell increase in the skin. In addition, it is unclear how the enrichment of mast cells provides protection against Bd infection and alternations to skin microbiomes after infection. It is important to determine whether skin mast cells release any contents mentioned above.

- https://doi.org/10.7554/eLife.92168.1.sa2

Reviewer #2 (Public Review):

Summary:
In this study, Hauser et al investigate the role of amphibian (Xenopus laevis) mast cells in cutaneous immune responses to the ecologically important pathogen Batrachochytrium dendrobatidis (Bd) using novel methods of in vitro differentiation of bone marrow-derived mast cells and in vivo expansion of skin mast cell populations. They find that bone marrow-derived myeloid precursors cultured in the presence of recombinant X. laevis Stem Cell Factor (rSCF) differentiate into cells that display hallmark characteristics of mast cells. They inject their novel (r)SCF reagent into the skin of X. laevis and find that this stimulates the expansion of cutaneous mast cell populations in vivo. They then apply this model of cutaneous mast cell expansion in the setting of Bd infection and find that mast cell expansion attenuates the skin burden of Bd zoospores and pathologic features including epithelial thickness and improves protective mucus production and transcriptional markers of barrier function. Utilizing their prior expertise with expanding neutrophil populations in X. laevis, the authors compare mast cell expansion using (r)SCF to neutrophil expansion using recombinant colony-stimulating factor 3 (rCSF3) and find that neutrophil expansion in Bd infection leads to greater burden of zoospores and worse skin pathology.

Strengths:
The authors report a novel method of expanding amphibian mast cells utilizing their custom-made rSCF reagent. They rigorously characterize expanded mast cells in vitro and in vivo using histologic, morphologic, transcriptional, and functional assays. This establishes solid footing with which to then study the role of rSCF-stimulated mast cell expansion in the Bd infection model. This appears to be the first demonstration of the exogenous use of rSCF in amphibians to expand mast cell populations and may set a foundation for future mechanistic studies of mast cells in the X. laevis model organism.

Weaknesses:
The conclusions regarding the role of mast cell expansion in controlling Bd infection would be stronger with a more rigorous evaluation of the model, as there are some key gaps and remaining questions regarding the data. For example:

1. Granulocyte expansion is carefully quantified in the initial time courses of rSCF and rCSF3 injections, but similar quantification is not provided in the disease models (Figures 3E, 4G, 5D-G). A key implication of the opposing effects of mast cell vs neutrophil expansion is that mast cells may suppress neutrophil recruitment or function. Alternatively, mast cells also express notable levels of csfr3 (Figure 2) and previous work from this group (Hauser et al, Facets 2020) showed rG-CSF-stimulated peritoneal granulocytes express mast cell markers including kit and tpsab1, raising the question of what effect rCSF3 might have on mast cell populations in the skin. Considering these points, it would be helpful if both mast cells and neutrophils were quantified histologically (based on Figure 1, they can be readily distinguished by SE or Giemsa stain) in the Bd infection models.

2. Epithelial thickness and inflammation in Bd infection are reported to be reduced by rSCF treatment (Figure 3E, 5A-B) or increased by rCSF3 treatment (Figure 4G) but quantification of these critical readouts is not shown.

3. Critical time points in the Bd model are incompletely characterized. Mast cell expansion decreases zoospore burden at 21 dpi, while there is no difference at 7 dpi (Figure 3E). Conversely, neutrophil expansion increases zoospore burden at 7 dpi, but no corresponding 21 dpi data is shown for comparison (Figure 4G). Microbiota analysis is performed at a third time point,10 dpi (Figure 5D-G), making it difficult to compare with the data from the 7 dpi and 21 dpi time points. Reporting consistent readouts at these three time points is important

to draw solid conclusions about the relationship of mast cell expansion to Bd infection and shifts in microbiota.

4. Although the effect of rSCF treatment on Bd zoospores is significant at 21 dpi (Figure 3E), bacterial microbiota changes at 21 dpi are not (Figure S3B-C). This discrepancy, how it relates to the bacterial microbiota changes at 10 dpi, and why 7, 10, and 21 dpi time points were chosen for these different readouts (Figure 5F-G), is not discussed.

5. The time course of rSCF or rCSF3 treatments relative to Bd infection in the experiments is not clear. Were the treatments given 12 hours prior to the final analysis point to maximize the effect? For example, in Figure 3E, were rSCF injections given at 6.5 dpi and 20.5 dpi? Or were treatments administered on day 0 of the infection model? If the latter, how do the authors explain the effects at 7 dpi or 21 dpi given mast cell and neutrophil numbers return to baseline within 24 hours after rSCF or rCSF3 treatment, respectively?

The title of the manuscript may be mildly overstated. Although Bd infection can indeed be deadly, mortality was not a readout in this study, and it is not clear from the data reported that expanding skin mast cells would ultimately prevent progression to death in Bd infections.

- https://doi.org/10.7554/eLife.92168.1.sa1

Reviewer #3 (Public Review):

Summary:
Hauser et al. provide an exceptional study describing the role of resident mast cells in amphibian epidermis that produce anti-inflammatory cytokines that prevent Batrachochytrium dendrobatidis (Bd) infection from causing harmful inflammation, and also protect frogs from changes in skin microbiomes and loss of mucin in glands and loss of mucus integrity that otherwise cause changes to their skin microbiomes. Neutrophils, in contrast, were not protective against Bd infection. Beyond the beautiful cytology and transcriptional profiling, the authors utilized elegant cell enrichment experiments to enrich mast cells by recombinant stem cell factor, or to enrich neutrophils by recombinant colony-stimulating factor-3, and examined respective infection outcomes in Xenopus.

Strengths:
Through the use of recombinant IL4, the authors were able to test and eliminate the hypothesis that mast cell production of IL4 was the mechanism of host protection from Bd infection. Instead, impacts on the mucus glands and interaction with the skin microbiome are implicated as the protective mechanism. These results will press disease ecologists to examine the relative importance of this immune defense among species, the influence of mast cells on the skin microbiome and mucosal function, and open the potential for modulating mucosal defense.

Weaknesses:
A reduction of bacterial diversity upon infection, as described at the end of the results section, may not always be an "adverse effect," particularly given that anti-Bd function of the microbiome increased. Some authors (see Letourneau et al. 2022 ISME, or Woodhams et al. 2023 DCI) consider these short-term alterations as encoding ecological memory, such that continued exposure to a pathogen would encounter an enriched microbial defense. Regardless, mast cell-initiated protection of the mucus layer may negate the need for this microbial memory defense.

While the description of the mast cell location in the epidermal skin layer in amphibians is novel, it is not known how representative these results are across species ranging in chytridiomycosis susceptibility. No management applications are provided such as methods

to increase this defense without the use of recombinant stem cell factor, and more discussion is needed on how the mast cell component (abundance, distribution in the skin) of the epidermis develops or is regulated.

- https://doi.org/10.7554/eLife.92168.1.sa0

Author Response:

> ***Reviewer #1 (Public Review):***
>
> *Summary:*
> *The global decline of amphibians is primarily attributed to deadly disease outbreaks caused by the chytrid fungus, Batrachochytrium dendrobatidis (Bd). It is unclear whether and how skin-resident immune cells defend against Bd. Although it is well known that mammalian mast cells are crucial immune sentinels in the skin and play a pivotal role in the immune recognition of pathogens and orchestrating subsequent immune responses, the roles of amphibian mast cells during Bd infections are largely unknown. The current study developed a novel way to enrich X. laevis skin mast cells by injecting the skin with recombinant stem cell factor (SCF), a KIT ligand required for mast cell differentiation and survival. The investigators found an enrichment of skin mast cells provides X. laevis substantial protection against Bd and mitigates the inflammation-related skin damage resulting from Bd infection. Additionally, the augmentation of mast cells leads to increased mucin content within cutaneous mucus glands and shields frogs from the alterations to their skin microbiomes caused by Bd.*
>
> *Strengths:*
> *This study underscores the significance of amphibian skin-resident immune cells in defenses against Bd and introduces a novel approach to examining interactions between amphibian hosts and fungal pathogens.*
>
> *Weaknesses:*
> *The main weakness of the study is the lack of functional analysis of X. laevis mast cells. Upon activation, mast cells have the characteristic feature of degranulation to release histamine, serotonin, proteases, cytokines, and chemokines, etc. The study should determine whether X. laevis mast cells can be degranulated by two commonly used mast cell activators IgE and compound 48/80 for IgE-dependent and independent pathways. This can be easily done in vitro. It is also important to assess whether in vivo these mast cells are degranulated upon Bd infection using avidin staining to visualize vesicle releases from mast cells. Figure 3 only showed rSCF injection caused an increase in mast cells in naïve skin. They need to present whether Bd infection can induce mast cell increase and rSCF injection under Bd infection causes a mast cell increase in the skin. In addition, it is unclear how the enrichment of mast cells provides protection against Bd infection and alternations to skin microbiomes after infection. It is important to determine whether skin mast cells release any contents mentioned above.*

We would like to thank the reviewer for taking the time to review our work and for providing us with valuable feedback.

Please note that amphibians do not possess the IgE antibody isotype1.

To our knowledge there have been no published studies using approaches for studying mammalian mast cell degranulation to examine amphibian mast cells. Notably, several studies suggest that amphibian mast cells lack histamine2, 3, 4, 5 and serotonin2, 6. While there are commercially available kits and reagents for examining mammalian mast cell granule content, most of these reagents may not cross-react with their amphibian

counterparts. This is especially true of cytokines and chemokines, which diverged quickly with evolution and thus do not share substantial protein sequence identity across species as divergent as frogs and mammals. Respectfully, while following up on these findings is possible, it would involve considerable additional work to find reagents that would detect amphibian mast cell contents.

We would also like to respectfully point out that while mast cell degranulation is a feature most associated with mammalian mast cells, this is not the only means by which mammalian mast cells confer their immunological effects. While we agree that defining the biology of amphibian mast cell degranulation is important, we anticipate that since the anti-*Bd* protection conferred by enriching frog mast cells is seen after 21 days of enrichment, it is quite possible that degranulation may not be the central mechanism by which the mast cells are mediating this protection.

As noted in our manuscript, frog mast cells upregulate their expression of interleukin-4 (IL4), which is a hallmark cytokine associated with mammalian mast cells7. We are presently exploring the role of the frog IL4 in the observed mast cell anti-*Bd* protection. Should we generate meaningful findings in this regard, we will add them to the revised version of this manuscript.

We are also exploring the heparin content of frog mast cells and capacities of these cells to degranulate *in vitro* in response to compound 48/80. In addition, we are exploring *in vivo* mast cell degranulation via histology and avidin-staining. Should these studies generate significant findings, we will include them in the revised version of this manuscript.

Per the reviewer's suggestion, in our revised manuscript we also plan to include data showing whether *Bd* infections affect skin mast cell numbers and how rSCF injection impacts skin mast cell numbers in the context of *Bd* infections.

In regard to how mast cells impact *Bd* infections and skin microbiomes, our data indicate that mast cells are augmenting skin integrity during *Bd* infections and promoting mucus production, as indicated by the findings presented in Figure 4A-C and Figure 5A-C, respectively. There are several mammalian mast cell products that elicit mucus production. In mammals, this mucus production is mediated by goblet cells while the molecular control of amphibian skin mucus gland content remains incompletely understood. Interleukin-13 (IL13) is the major cytokine associated with mammalian mucus production8, while to our knowledge this cytokine is either not encoded by amphibians or else has yet to be identified and annotated in these animals' genomes. IL4 signaling also results in mucus production9 and we are presently exploring the possible contribution of the *X. laevis* IL4 to skin mucus gland filling. Any significant findings on this front will be included in the revised manuscript. Histamine release contributes to mast cell-mediated mucus production10, but as we outline above, several studies indicate that amphibian mast cells may lack histamine2, 3, 4, 5. Mammalian mast cell-produced lipid mediators also play a critical role in eliciting mucus secretion11 and our transcriptomic analysis indicates that frog mast cells express several enzymes associated with production of such mediators. We will highlight this observation in our revised manuscript.

We anticipate that *X. laevis* mast cells influence skin integrity, microbial composition and *Bd* susceptibility in a myriad of ways. Considering the substantial differences between amphibian and mammalian evolutionary histories and physiologies, we anticipate that many of the mechanisms by which *X. laevis* mast cells confer anti-*Bd* protection will prove to be specific to amphibians and some even unique to *X. laevis*. We are most interested in deciphering what these mechanisms are but foresee that they will not necessarily reflect what one would expect based on what we know about mammalian mast cells in the context of mammalian physiologies.

Reviewer #2 (Public Review):

Summary:
In this study, Hauser et al investigate the role of amphibian (Xenopus laevis) mast cells in cutaneous immune responses to the ecologically important pathogen Batrachochytrium dendrobatidis (Bd) using novel methods of in vitro differentiation of bone marrow-derived mast cells and in vivo expansion of skin mast cell populations. They find that bone marrow-derived myeloid precursors cultured in the presence of recombinant X. laevis Stem Cell Factor (rSCF) differentiate into cells that display hallmark characteristics of mast cells. They inject their novel (r)SCF reagent into the skin of X. laevis and find that this stimulates the expansion of cutaneous mast cell populations in vivo. They then apply this model of cutaneous mast cell expansion in the setting of Bd infection and find that mast cell expansion attenuates the skin burden of Bd zoospores and pathologic features including epithelial thickness and improves protective mucus production and transcriptional markers of barrier function. Utilizing their prior expertise with expanding neutrophil populations in X. laevis, the authors compare mast cell expansion using (r)SCF to neutrophil expansion using recombinant colony-stimulating factor 3 (rCSF3) and find that neutrophil expansion in Bd infection leads to greater burden of zoospores and worse skin pathology.

Strengths:
The authors report a novel method of expanding amphibian mast cells utilizing their custom-made rSCF reagent. They rigorously characterize expanded mast cells in vitro and in vivo using histologic, morphologic, transcriptional, and functional assays. This establishes solid footing with which to then study the role of rSCF-stimulated mast cell expansion in the Bd infection model. This appears to be the first demonstration of the exogenous use of rSCF in amphibians to expand mast cell populations and may set a foundation for future mechanistic studies of mast cells in the X. laevis model organism.

We thank the reviewer for recognizing the breadth and extent of the undertaking that culminated in this manuscript. Indeed, this manuscript would not have been possible without considerable reagent development and adaptation of techniques that had previously not been used for amphibian immunity research. In line with the reviewer's sentiment, to our knowledge this is the first report of using molecular approaches to augment amphibian mast cells, which we hope will pave the way for new areas of research within the fields of comparative immunology and amphibian disease biology.

Weaknesses:
The conclusions regarding the role of mast cell expansion in controlling Bd infection would be stronger with a more rigorous evaluation of the model, as there are some key gaps and remaining questions regarding the data. For example:

1. Granulocyte expansion is carefully quantified in the initial time courses of rSCF and rCSF3 injections, but similar quantification is not provided in the disease models (Figures 3E, 4G, 5D-G). A key implication of the opposing effects of mast cell vs neutrophil expansion is that mast cells may suppress neutrophil recruitment or function. Alternatively, mast cells also express notable levels of csfr3 (Figure 2) and previous work from this group (Hauser et al, Facets 2020) showed rG-CSF-stimulated peritoneal granulocytes express mast cell markers including kit and tpsab1, raising the question of what effect rCSF3 might have on mast cell populations in the skin. Considering these points, it would be helpful if both mast cells and neutrophils were quantified histologically (based on Figure 1, they can be readily distinguished by SE or Giemsa stain) in the Bd infection models.

We thank the reviewer for this insightful suggestion. We are performing a further examination of skin granulocyte content during *Bd* infections and plan on including any significant findings in our revised manuscript.

We predict that rSCF administration results in the accumulation of mast cells that are polarized such that they ablate the inflammatory response elicited by *Bd* infection. Mammalian mast cells, including peritonea-resident mast cells, express csf3r12, 13. Although the *X. laevis* animal model does not permit nearly the degree of immune cell resolution afforded by mammalian animal models, we do know that the adult *X. laevis* peritonea contain heterogenous leukocyte populations. We anticipate that the high kit expression reported by Hauser *et al.,* 2020 in the rCSF3-recruited peritoneal leukocytes reflects the presence of mast cells therein. As such and in acknowledgement of the reviewer's suggestion, we also think that the cells recruited by rCSF3 into the skin may include not only neutrophils but also mast cells. Possibly, these mast cells have distinct polarization states from those enriched by rSCF. While the lack of antibodies against frog neutrophils or mast cells has limited our capacity to address this question, we will attempt to reexamine by histology the proportions of skin neutrophils and mast cells in the skins of frogs under the conditions described in our manuscript. Any new findings in this regard will be included in the revised version of this work.

> *2. Epithelial thickness and inflammation in Bd infection are reported to be reduced by rSCF treatment (Figure 3E, 5A-B) or increased by rCSF3 treatment (Figure 4G) but quantification of these critical readouts is not shown.*

We thank the reviewer for this suggestion. We will score epithelial thickness under the distinct conditions described in our manuscript and present the quantified data in the revised paper.

> *3. Critical time points in the Bd model are incompletely characterized. Mast cell expansion decreases zoospore burden at 21 dpi, while there is no difference at 7 dpi (Figure 3E). Conversely, neutrophil expansion increases zoospore burden at 7 dpi, but no corresponding 21 dpi data is shown for comparison (Figure 4G). Microbiota analysis is performed at a third time point,10 dpi (Figure 5D-G), making it difficult to compare with the data from the 7 dpi and 21 dpi time points. Reporting consistent readouts at these three time points is important to draw solid conclusions about the relationship of mast cell expansion to Bd infection and shifts in microbiota.*

Because there were no significant effects of mast cell enrichment at 7 days post *Bd* infection, we chose to look at the microbiome composition in a subsequent experiment at 10 days and 21 days post *Bd* infection, with 10 days being a bit more of a midway point between the initial exposure and day 21, when we see the effect on *Bd* loads. We will clarify this rationale in the revised manuscript.

The enrichment of neutrophils in frog skins resulted in prompt (12 hours post enrichment) skin thickening (in absence of *Bd* infection) and increased frog *Bd* susceptibility by 7 days of infection. Conversely, mast cell enrichment stabilized skin mucosal and symbiotic microbial environment, presumably accounting at least in part for the lack of further *Bd* growth on mast cell-enriched animals by 21 days of infection. Our question regarding the roles of inflammatory granulocytes/neutrophils during *Bd* infections was that of 'how' rather 'when' these cells affect *Bd* infections. Because the central focus of this work was mast cells and not other granulocyte subsets, when we saw that rCSF3-recruited granulocytes adversely affected *Bd* infections at 7 days post infection, we did not pursue the kinetics of these responses further. We plan to explore the roles of inflammatory mediators and disparate frog immune cell subsets during the course of *Bd* infections, but we feel that these future studies are more

peripheral to the central thesis of the present manuscript regarding the roles of frog mast cells during *Bd* infections.

> *4. Although the effect of rSCF treatment on Bd zoospores is significant at 21 dpi (Figure 3E), bacterial microbiota changes at 21 dpi are not (Figure S3B-C). This discrepancy, how it relates to the bacterial microbiota changes at 10 dpi, and why 7, 10, and 21 dpi time points were chosen for these different readouts (Figure 5F-G), is not discussed.*

Our results indicate that after 10 days of *Bd* infection, control *Bd*-challenged animals exhibited reduced microbial richness, while skin mast cell-enriched *Bd*-infected frogs were protected from this disruption of their microbiome. The amphibian microbiome serves as a major barrier to these fungal infections14, and we anticipate that *Bd*-mediated disruption of microbial richness and composition facilitates host skin colonization by this pathogen. Control and mast cell-enriched animals had similar skin *Bd* loads at 10 days post infection. However, by 21 days of *Bd* infection the mast cells-enriched animals maintained their *Bd* loads to levels observed at 10 days post infection, whereas the control animals had significantly greater *Bd* loads. Thus, we anticipate that frog mast cells are conferring the observed anti-*Bd* protection in part by preventing microbial disassembly and thus interfering with optimal *Bd* colonization and growth on frog skins. In other words, maintained microbial composition at 10 days of infection may be preventing additional *Bd* colonization/growth, as seen when comparing skins of control and mast cell-enriched frogs at 21 days post infection. By 21 days of infection, control animals rebounded from the *Bd*-mediated reduction in bacterial richness seen at 10 days. Considering that after 21 days of infection control animals also had significantly greater *Bd* loads than mast-cell enriched animals suggests that there may be a critical earlier window during which microbial composition is able to counteract _Bd_growth.

While the current draft of our manuscript has a paragraph to this effect (see below), we appreciate the reviewer conveying to us that our perspective on the relationship between skin mast cells and the kinetics of microbial composition and _Bd_loads could be better emphasized. We plan to revise our manuscript to include the above discussion points.

Bd infections caused major reductions in bacterial taxa richness, changes in composition and substantial increases in the relative abundance of *Bd*-inhibitory bacteria early in the infection. Similar changes to microbiome structure occur during experimental *Bd* infections of red-backed salamanders and mountain yellow-legged frogs15, 16. In turn, progressing _Bd_infections corresponded with a return to baseline levels of *Bd*-inhibitory bacteria abundance and rebounding microbial richness, albeit with dissimilar communities to those seen in control animals. These temporal changes indicate that amphibian microbiomes are dynamic, as are the effects of *Bd* infections on them. Indeed, *Bd* infections may have long-lasting impacts on amphibian microbiomes15. While *Bd* infections manifested in these considerable changes to frog skin microbiome structure, mast cell enrichment appeared to counteract these deleterious effects to their microbial composition. Presumably, the greater skin mucosal integrity and mucus production observed after mast cell enrichment served to stabilize the cutaneous environment during *Bd* infections, thereby ameliorating the *Bd*-mediated microbiome changes. While this work explored the changes in established antifungal flora, we anticipate the mast cell-mediated inhibition of *Bd* may be due to additional, yet unidentified bacterial or fungal taxa. Intriguingly, while mammalian skin mast cell functionality depends on microbiome elicited SCF production by keratinocytes17, our results indicate that frog skin mast cells in turn impact skin microbiome structure and likely their function. It will be interesting to further explore the interdependent nature of amphibian skin microbiomes and resident mast cells.

> *5. The time course of rSCF or rCSF3 treatments relative to Bd infection in the experiments is not clear. Were the treatments given 12 hours prior to the final analysis point to*

> *maximize the effect? For example, in Figure 3E, were rSCF injections given at 6.5 dpi and 20.5 dpi? Or were treatments administered on day 0 of the infection model? If the latter, how do the authors explain the effects at 7 dpi or 21 dpi given mast cell and neutrophil numbers return to baseline within 24 hours after rSCF or rCSF3 treatment, respectively?*

Please find the schematic of the immune manipulation, *Bd* infection, and sample collection times below. We will include a figure like this in our revised manuscript.

> *The title of the manuscript may be mildly overstated. Although Bd infection can indeed be deadly, mortality was not a readout in this study, and it is not clear from the data reported that expanding skin mast cells would ultimately prevent progression to death in Bd infections.*

We acknowledge this point. The revised manuscript will be titled: “Amphibian mast cells: barriers to chytrid fungus infections”.

> ***Reviewer #3 (Public Review):***
>
> *Summary:*
> *Hauser et al. provide an exceptional study describing the role of resident mast cells in amphibian epidermis that produce anti-inflammatory cytokines that prevent Batrachochytrium dendrobatidis (Bd) infection from causing harmful inflammation, and also protect frogs from changes in skin microbiomes and loss of mucin in glands and loss of mucus integrity that otherwise cause changes to their skin microbiomes. Neutrophils, in contrast, were not protective against Bd infection. Beyond the beautiful cytology and transcriptional profiling, the authors utilized elegant cell enrichment experiments to enrich mast cells by recombinant stem cell factor, or to enrich neutrophils by recombinant colony-stimulating factor-3, and examined respective infection outcomes in Xenopus.*
>
> *Strengths:*
> *Through the use of recombinant IL4, the authors were able to test and eliminate the hypothesis that mast cell production of IL4 was the mechanism of host protection from Bd infection. Instead, impacts on the mucus glands and interaction with the skin microbiome are implicated as the protective mechanism. These results will press disease ecologists to examine the relative importance of this immune defense among species, the influence of mast cells on the skin microbiome and mucosal function, and open the potential for modulating mucosal defense.*

We thank the reviewer for recognizing the significance and utility of the findings presented in our manuscript.

> *Weaknesses:*
> *A reduction of bacterial diversity upon infection, as described at the end of the results section, may not always be an "adverse effect," particularly given that anti-Bd function of the microbiome increased. Some authors (see Letourneau et al. 2022 ISME, or Woodhams et al. 2023 DCI) consider these short-term alterations as encoding ecological memory, such that continued exposure to a pathogen would encounter an enriched microbial defense. Regardless, mast cell-initiated protection of the mucus layer may negate the need for this microbial memory defense.*

We thank the reviewer their insightful comment. We will revise our discussion to include this possible interpretation.

> *While the description of the mast cell location in the epidermal skin layer in amphibians is novel, it is not known how representative these results are across species ranging in chytridiomycosis susceptibility. No management applications are provided such as methods to increase this defense without the use of recombinant stem cell factor, and more discussion is needed on how the mast cell component (abundance, distribution in the skin) of the epidermis develops or is regulated.*

We appreciate the reviewer's comment and would like to point out that the work presented in our manuscript was driven by comparative immunology questions more than by conservation biology.

We thank the reviewer for suggesting expanding our discussion to include potential management applications and potential mechanisms for regulating frog skin mast cells. While any content to these effects would be highly speculative, we agree that it may spark new interest and pave new avenues for research. To this end, our revised manuscript will include a paragraph to this effect.

References:

1. Flajnik, M.F. A cold-blooded view of adaptive immunity. _Nat Rev Immunol_ 18, 438-453 (2018).
2. Mulero, I., Sepulcre, M.P., Meseguer, J., Garcia-Ayala, A. & Mulero, V. Histamine is stored in mast cells of most evolutionarily advanced fish and regulates the fish inflammatory response. _Proc Natl Acad Sci U S A_ 104, 19434-19439 (2007).
3. Reite, O.B. A phylogenetical approach to the functional significance of tissue mast cell histamine. _Nature_ 206, 1334-1336 (1965).
4. Reite, O.B. Comparative physiology of histamine. _Physiol Rev_ 52, 778-819 (1972).
5. Takaya, K., Fujita, T. & Endo, K. Mast cells free of histamine in Rana catasbiana. _Nature_ 215, 776-777 (1967).
6. Galli, S.J. New insights into "the riddle of the mast cells": microenvironmental regulation of mast cell development and phenotypic heterogeneity. _Lab Invest_ 62, 5-33 (1990).
7. Babina, M., Guhl, S., Artuc, M. & Zuberbier, T. IL-4 and human skin mast cells revisited: reinforcement of a pro-allergic phenotype upon prolonged exposure. _Archives of dermatological research_ 308, 665-670 (2016).
8. Lai, H. & Rogers, D.F. New pharmacotherapy for airway mucus hypersecretion in asthma and COPD: targeting intracellular signaling pathways. _J Aerosol Med Pulm Drug Deliv_ 23, 219-231 (2010).
9. Rankin, J.A. _et al._ Phenotypic and physiologic characterization of transgenic mice expressing interleukin 4 in the lung: lymphocytic and eosinophilic inflammation without airway hyperreactivity. _Proc Natl Acad Sci U S A_ 93, 7821-7825 (1996).

10. Church, M.K. Allergy, Histamine and Antihistamines. _Handb Exp Pharmacol_ 241, 321-331 (2017).

11. Nakamura, T. The roles of lipid mediators in type I hypersensitivity. _J Pharmacol Sci_ 147, 126-131 (2021).

12. Aponte-Lopez, A., Enciso, J., Munoz-Cruz, S. & Fuentes-Panana, E.M. An In Vitro Model of Mast Cell Recruitment and Activation by Breast Cancer Cells Supports Anti-Tumoral Responses. _Int J Mol Sci_ 21 (2020).

13. Jamur, M.C. _et al._ Mast cell repopulation of the peritoneal cavity: contribution of mast cell progenitors versus bone marrow derived committed mast cell precursors. _BMC Immunol_ 11, 32 (2010).

14. Walke, J.B. & Belden, L.K. Harnessing the Microbiome to Prevent Fungal Infections: Lessons from Amphibians. _PLoS Pathog_ 12, e1005796 (2016).

15. Jani, A.J. _et al._ The amphibian microbiome exhibits poor resilience following pathogen-induced disturbance. _ISME J_ 15, 1628-1640 (2021).

16. Muletz-Wolz, C.R., Fleischer, R.C. & Lips, K.R. Fungal disease and temperature alter skin microbiome structure in an experimental salamander system. _Mol Ecol_ 28, 2917-2931 (2019).

17. Wang, Z. _et al._ Skin microbiome promotes mast cell maturation by triggering stem cell factor production in keratinocytes. _J Allergy Clin Immunol_ 139, 1205-1216 e1206 (2017).